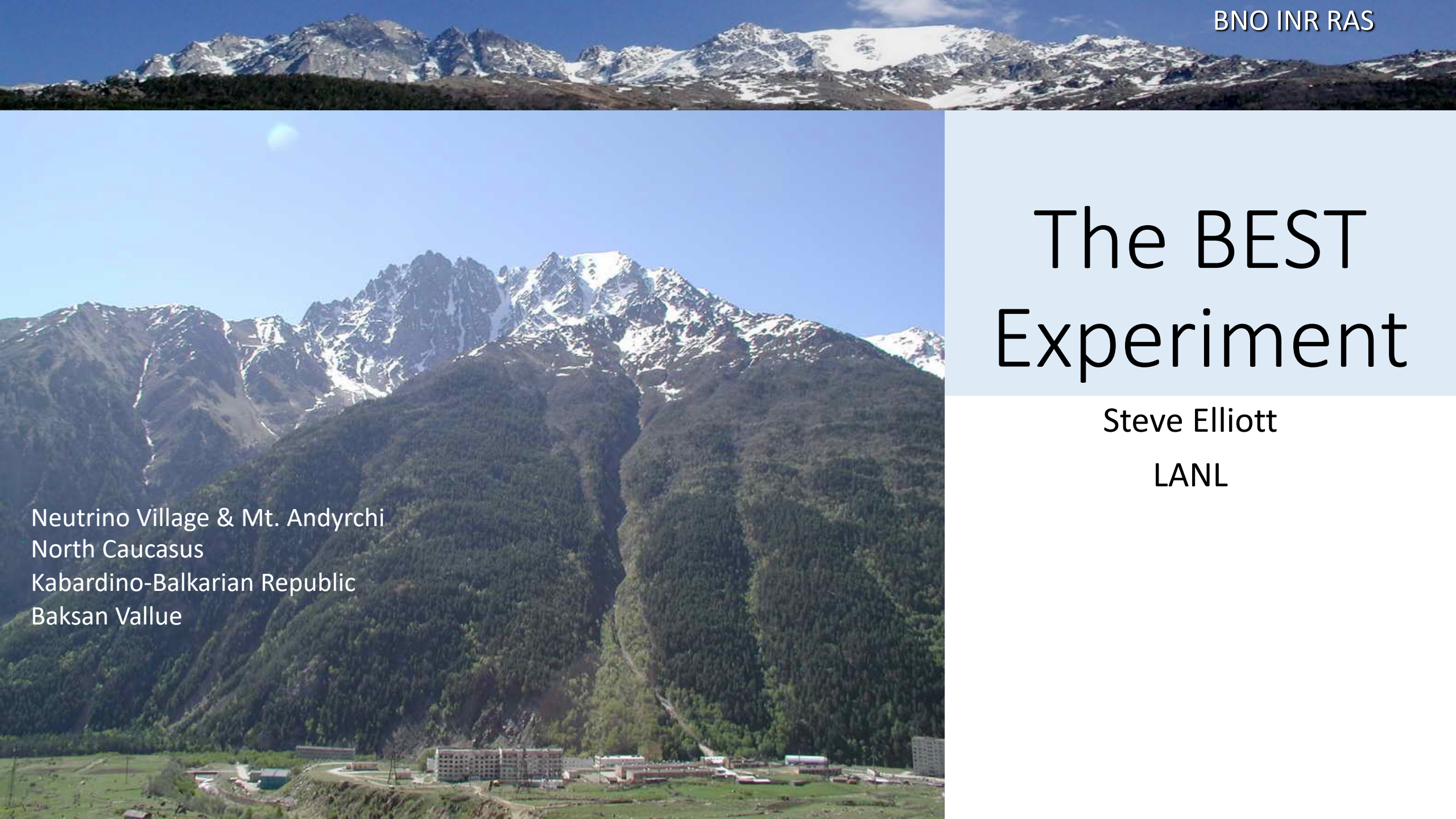# The BEST Experiment

Steve Elliott

LANL

Neutrino Village & Mt. Andyrchi
North Caucasus
Kabardino-Balkarian Republic
Baksan Vallue

Baksan Experiment on Sterile Transitions (BEST)

arXiv:2109.11482
Spokesperson – Vladimir Gavrin

V.V. Barinov,[1] B.T. Cleveland,[2] S.N. Danshin,[1] H. Ejiri,[3] S.R. Elliott,[4] D. Frekers,[5] V.N. Gavrin,[1,a]
V.V. Gorbachev,[1] D.S. Gorbunov,[1] W.C. Haxton,[6,7] T.V. Ibragimova,[1] I. Kim,[4] Yu.P. Kozlova,[1]
L.V. Kravchuk,[1] V.V. Kuzminov,[1] B.K. Lubsandorzhiev,[1] Yu.M. Malyshkin,[1] R. Massarczyk,[4]
V.A. Matveev,[8] I.N. Mirmov,[1] J.S. Nico,[9] A.L. Petelin,[10] R.G.H. Robertson,[11] D. Sinclair,[12]
A.A. Shikhin,[1] V.A. Tarasov,[10] G.V. Trubnikov,[8] E.P. Veretenkin,[1] J.F. Wilkerson,[13,14] and A.I. Zvir[10]

[1] *Institute for Nuclear Research of the Russian Academy of Sciences, Moscow 117312, Russia*
[2] *SNOLAB, Sudbury, ON P3Y 1N2, Canada*
[3] *Research Center for Nuclear Physics, Osaka University, Osaka, Japan*
[4] *Los Alamos National Laboratory, Los Alamos, NM, USA*
[5] *Institut für Kernphysik, Westfälische Wilhelms-Universität Munster, D-48149 Munster, Germany*
[6] *Nuclear Science Division, Lawrence Berkeley National Laboratory, Berkeley, CA 94720, USA*
[7] *Department of Physics, University of California, Berkeley, CA 94720, USA*
[8] *Joint Institute for Nuclear Research (JINR) Joliot-Curie 6, 141980, Dubna, Moscow Region, Russia*
[9] *National Institute of Standards and Technology, 100 Bureau Dr, Gaithersburg, MD 20899, USA*
[10] *JSC 'State Scientific Center Research Institute of Atomic Reactors', Dimitrovgrad, 433510, Russia*
[11] *Center for Experimental Nuclear Physics and Astrophysics, and
Department of Physics, University of Washington, Seattle, WA 98195, USA*
[12] *Carleton University 1125 Colonel By Drive Ottawa, K1S 5B6, Canada*
[13] *Department of Physics and Astronomy, University of North Carolina, Chapel Hill, NC 27599, USA*
[14] *Triangle Universities Nuclear Laboratory, Durham, NC 27708, USA*

Overview of BEST

- Neutrinos produced at center of Ga by ^{51}Cr decay:

$$^{51}Cr + e^- \rightarrow {}^{51}V + \nu_e$$
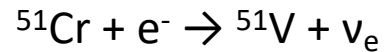
- This is a well-understood monochromatic spectrum of a compact source. The source intensity is well measured.

- These neutrinos are detected via a charged-current (CC) reaction on Ga surrounding the source:

$$\nu_e + {}^{71}Ga \rightarrow {}^{71}Ge + e^-$$
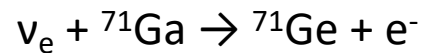
- Very Short Baseline. ~1m, two zone target to measure ν interaction rate at two distances.

- Almost zero background. Mainly from the Sun.

    The source, 3.4 MCi, provides a capture rate in the Ga that exceeds the rate from the Sun by several factors of ten.

- Well established experimental procedures for extraction and counting of the ^{71}Ge developed in SAGE solar measurements.

- Simple interpretation of results. (Phys. Part. Nucl. 46 (2015) 131)
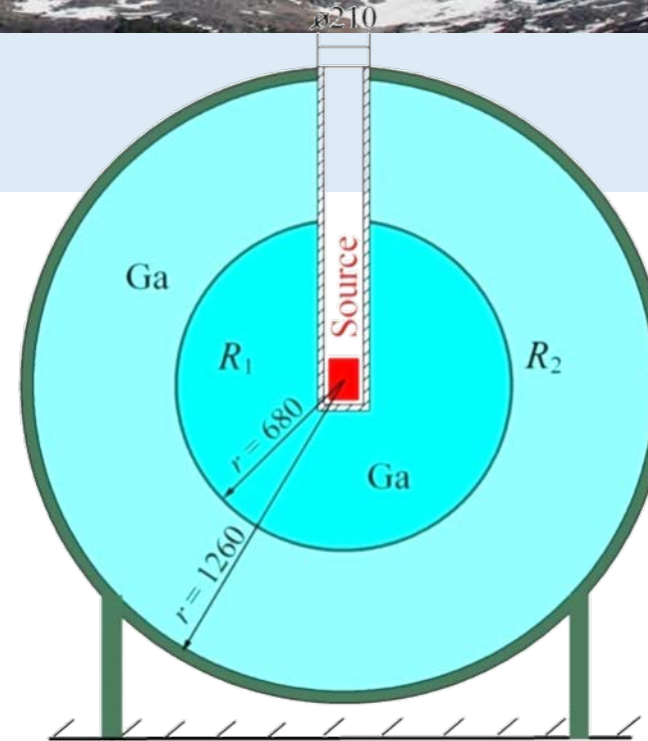
Schematic drawing of the BEST neutrino source experiment.
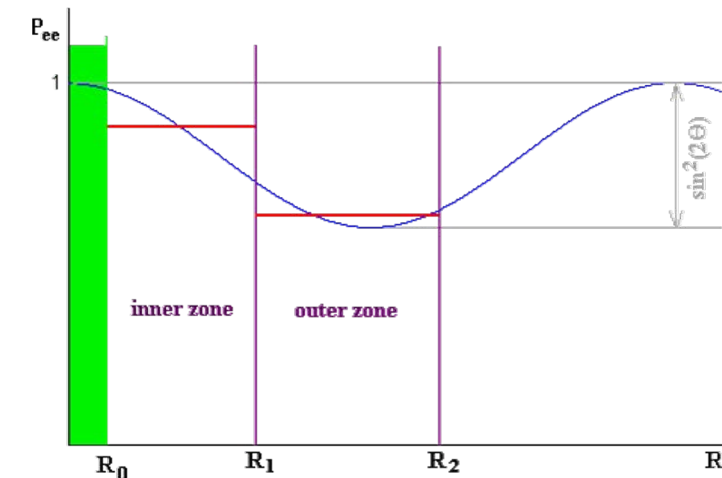
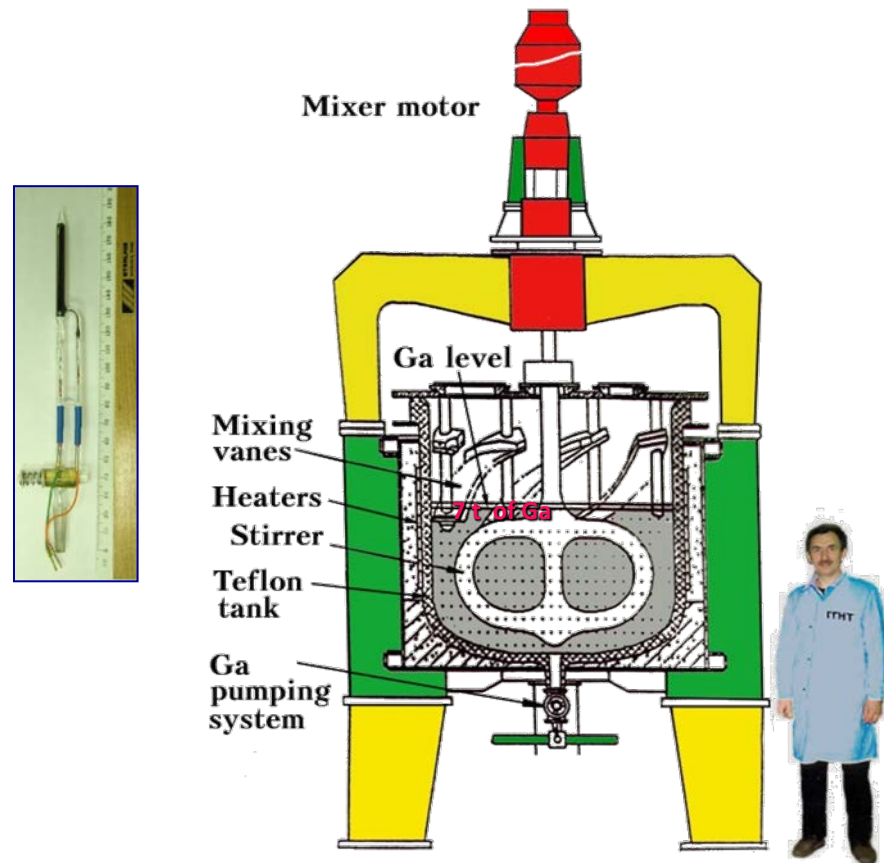# The Gallium Solar Neutrino Experiments (Kuzmin Eksp. Teor. Fiz. 49 (1965) 1532)

SAGE 50 t of Ga

Mixer motor
Ga level
Mixing vanes
Heaters
Stirrer
Teflon tank
Ga pumping system
7 t of Ga

Both experiments were based on radio-chemical extraction technology of a few ^{71}Ge atoms from tons of a Ga target and on technology of counting of ^{71}Ge decays in small proportional counters (~0.5 cm^3).

GALLEX/GNO 30.3 t of Ga

HD-II proportional counter
Gas inlet
Stopcock
Mercury
Front window
Anode wire (13 μ)
Active volume (1 cm)

N_2
$N_2 + GeCl_4$
H_2O
$GaCl_3$ + HCl
^{51}Cr
(54 m^3, 110 t)
H_2O + $GeCl_4$
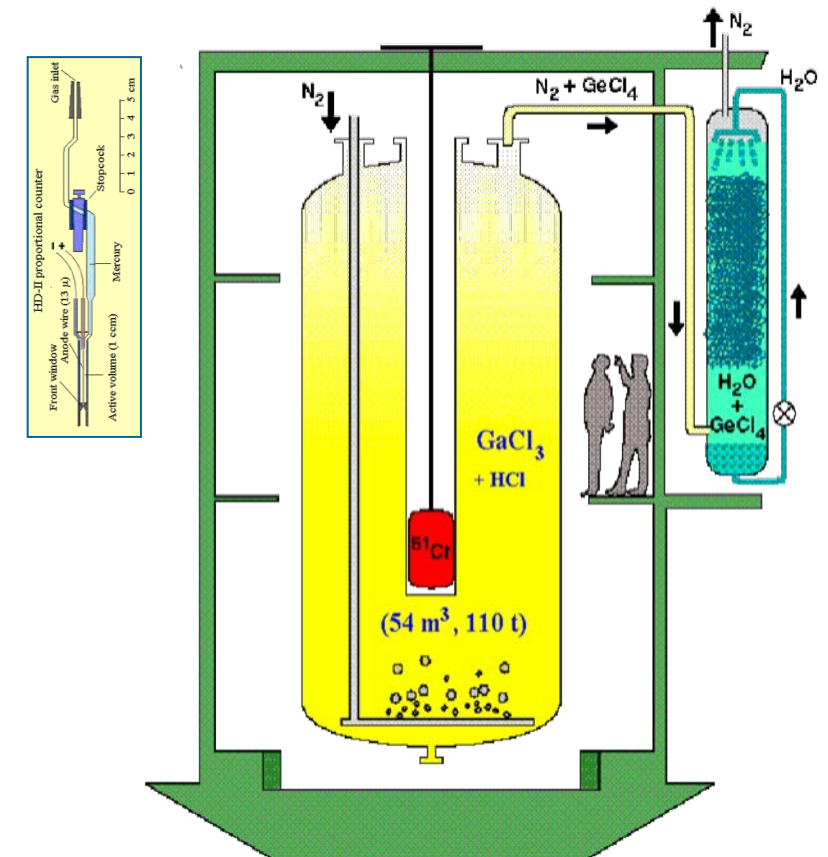
SAGE and GALLEX Results for Solar Neutrinos

SAGE/GALLEX/GNO: 66.1 ± 3.1 SNU (PRC 80 (2009) 015807)

Direct evidence for the p-p chain reactions for solar neutrino production in the Sun.

SAGE: 1990 – 2007

GALLEX/GNO: 1991 - 2003
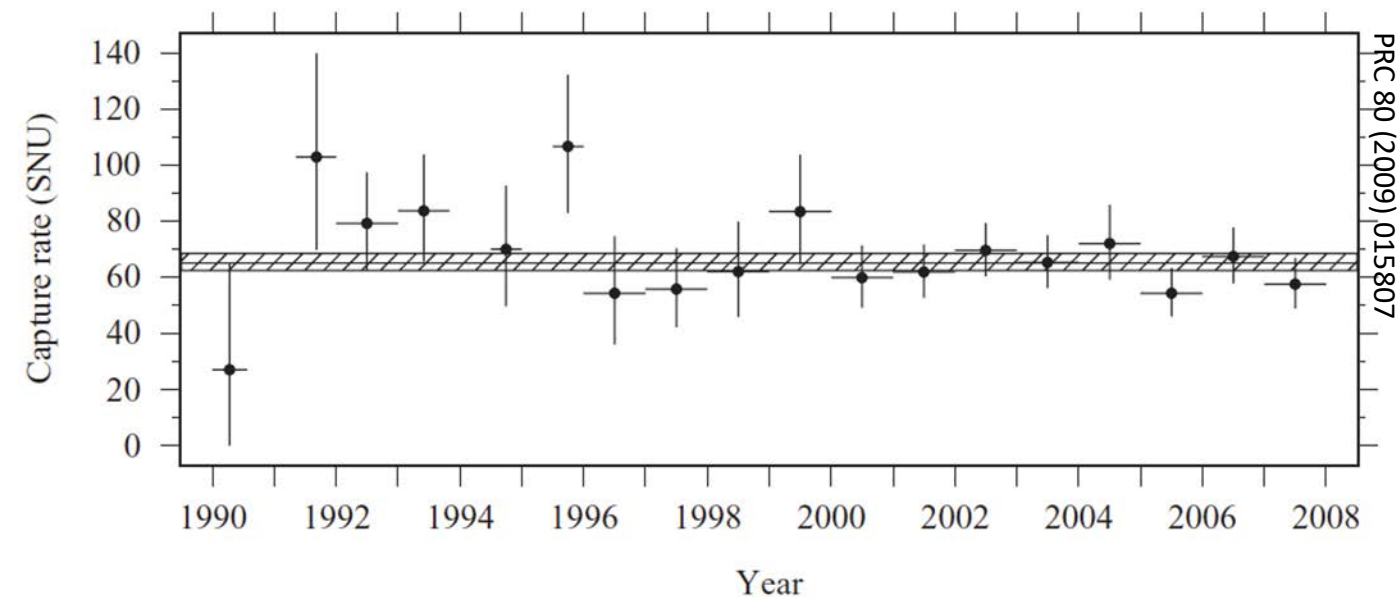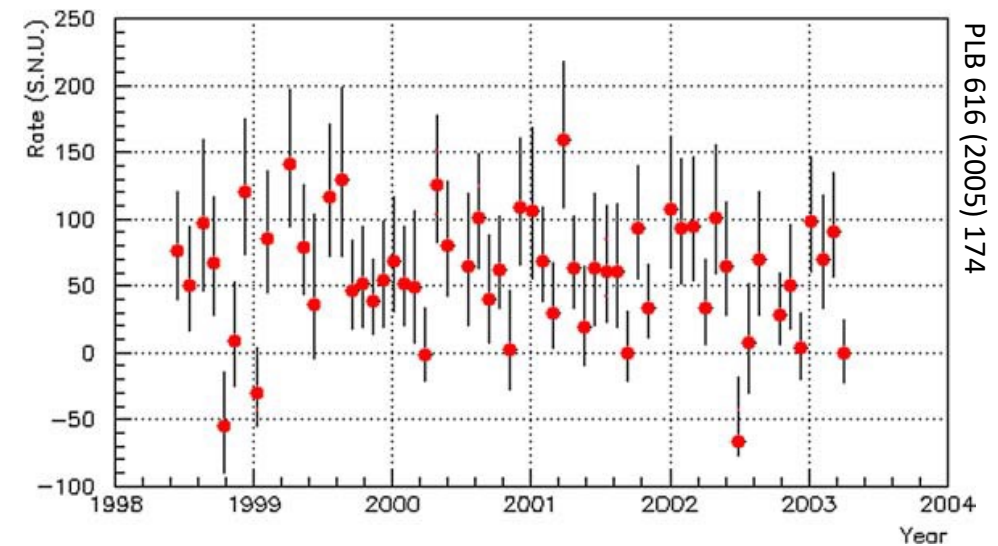

(**1 SNU** = 1 interaction/s in a target that contains 10^{36} atoms of the neutrino absorbing isotope).

SAGE and GALLEX Neutrino Source Experiments

Neutrino sources:

^{51}Cr: 747 keV (81.6%), 427 keV (9.0%), 752 keV (8.5%), 432 keV (0.9%)

^{37}Ar: 811 keV (90.2%), 813 keV (9.8%)

GALLEX:

| 1994 –1995 | $A(\text{Cr}_1) = 1.714 \pm 0.036$ MCi |
| 1995 –1996 | $A(\text{Cr}_2) = 1.868 \pm 0.073$ MCi |

SAGE:

| 1994 –1995 | $A(\text{Cr}) = 0.517 \pm 0.006$ MCi |
| 2004 | $A(\text{Ar}) = 0.409 \pm 0.002$ MCi |

Results:

GALLEX:

| PLB 342 (1995) | $R_1(\text{Cr}) = 0.953 \pm 0.11$ |
| PLB 420 (1998) | $R_2(\text{Cr}) = 0.812 \pm 0.10$ |

SAGE:

| PRC 59 (1999) | $R_3(\text{Cr}) = 0.95 \pm 0.12$ |
| PRC 73 (2006) | $R_4(\text{Ar}) = 0.791 \pm 0.084$ |

R – ratio of the measured production rate to that expected from the cross section (PRC 56 (1997) 3391) (no uncertainty on cross section included)

The Ga Anomaly

Previously measured rates of $^{71}Ga(\nu_e,e)^{71}Ge$ are lower than that predicted from the known cross section and ν_e flux. R=0.87±0.05

The ν_e sources in these experiments were the electron-capture isotopes, ^{51}Cr or ^{37}Ar.
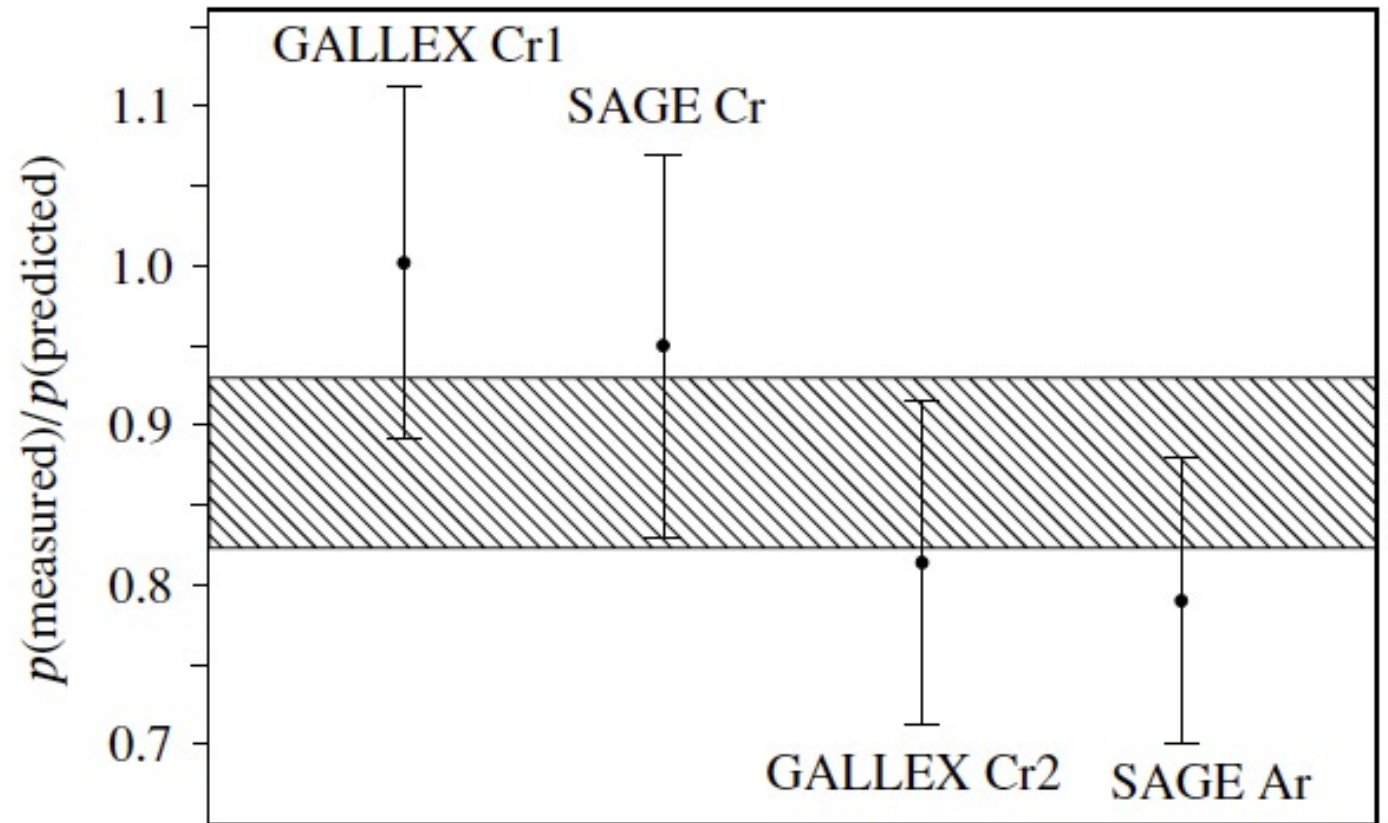
The Ga Anomaly has been considered evidence for sterile neutrinos (ν_s)

The decreased rate of ν_e detection has been interpreted with the hypothesis that the ν_e are oscillating into undetected ν_s.
$E_\nu \sim 1$ MeV, $L \sim 1$ m.

$$P_{ee}(E_\nu, r) = 1 - \sin^2 2\theta \sin^2\left(1.27 \frac{\Delta m^2 [\text{eV}^2] r [\text{m}]}{E_\nu [\text{MeV}]}\right)$$

Best fits tend toward high Δm^2 and $\sin^2 2\theta$.

Some references
PRD 78 (2008) 073009, PLB 795 (2019) 542, arXiv:2001.10064, PRD 86 (2012) 113014, NP B168 Proc. Supp. (2007) 344, PRD 97 (2018) 073001, NP B235 Proc. Supp. (2013) 214, J. Phys. G: Nucl. Part. Phys. 43 (2016) 033001
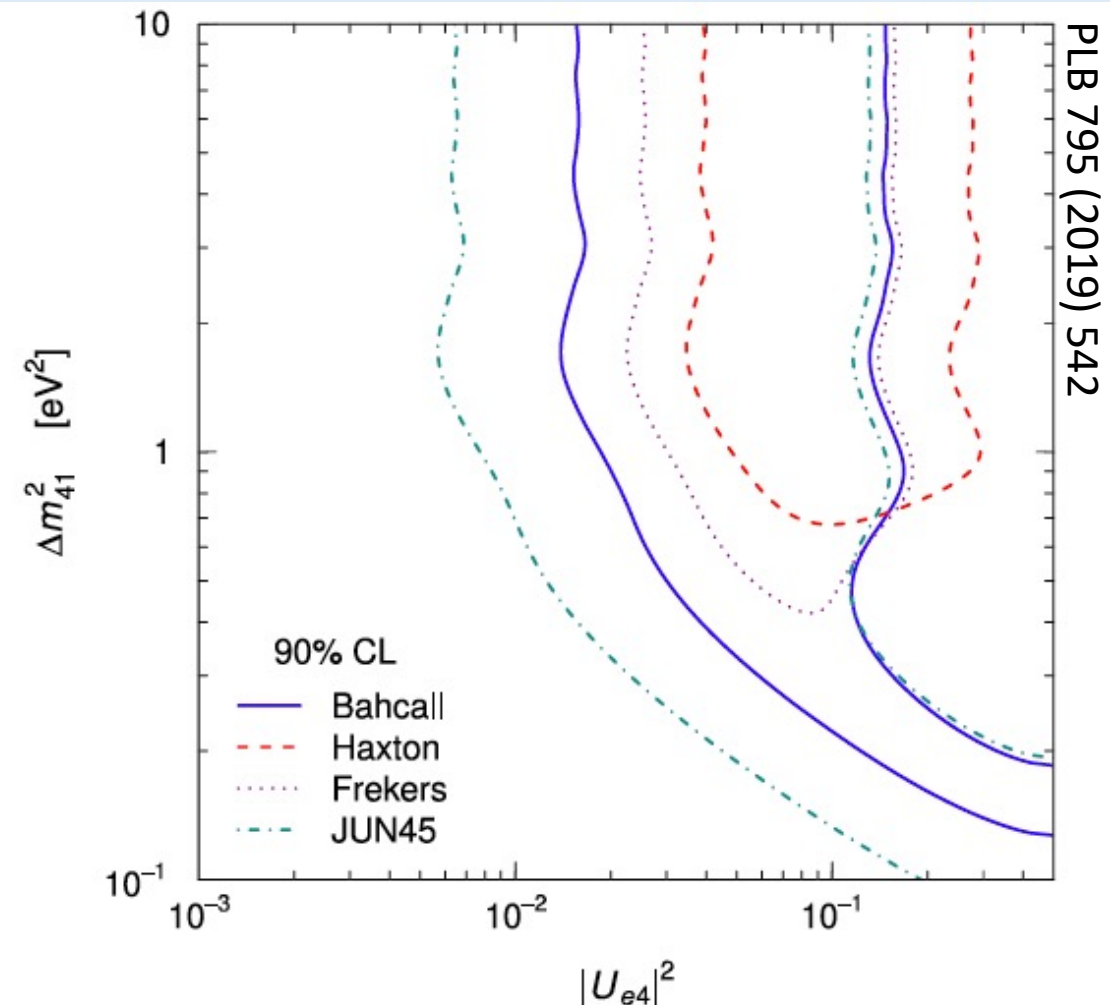
BEST Schedule

Construction began 2011
Source Arrived: July 5, 2019
Exposures: July 5 – Oct. 13, 2019
Counting: July 16, 2019 – Mar. 20, 2020
Counter Calibration: Mar. 2020 – Jan. 2021
PRL draft posted: Sept. 2021
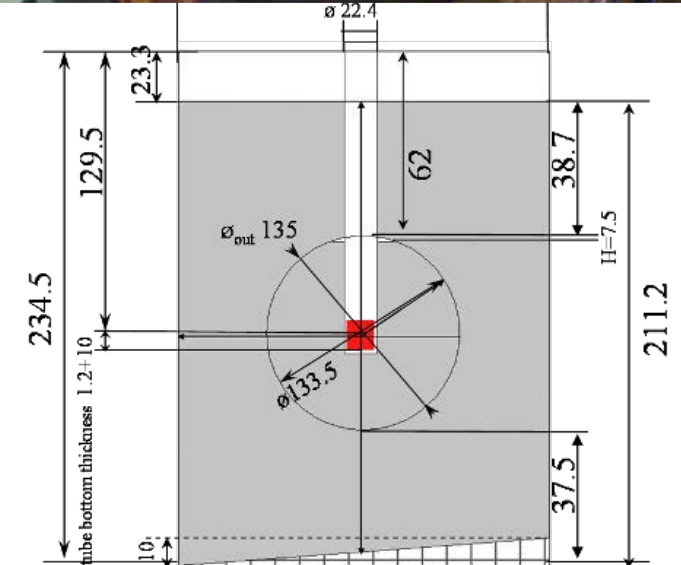
Construction started in 2011

2-Zone Gallium Target

Calorimeter

Lead chamber

Source

Installation and Operation

1. Expose gallium targets to the source
$$\nu_e + {}^{71}Ga \rightarrow {}^{71}Ge + e^-$$

2. Pump Ga to the chemical reactors

3. ${}^{71}Ge$ chemical extraction

4. ${}^{71}Ge$ decay measurement in proportional counters

5. Semiconductor & Calorimetric measurement for source activity
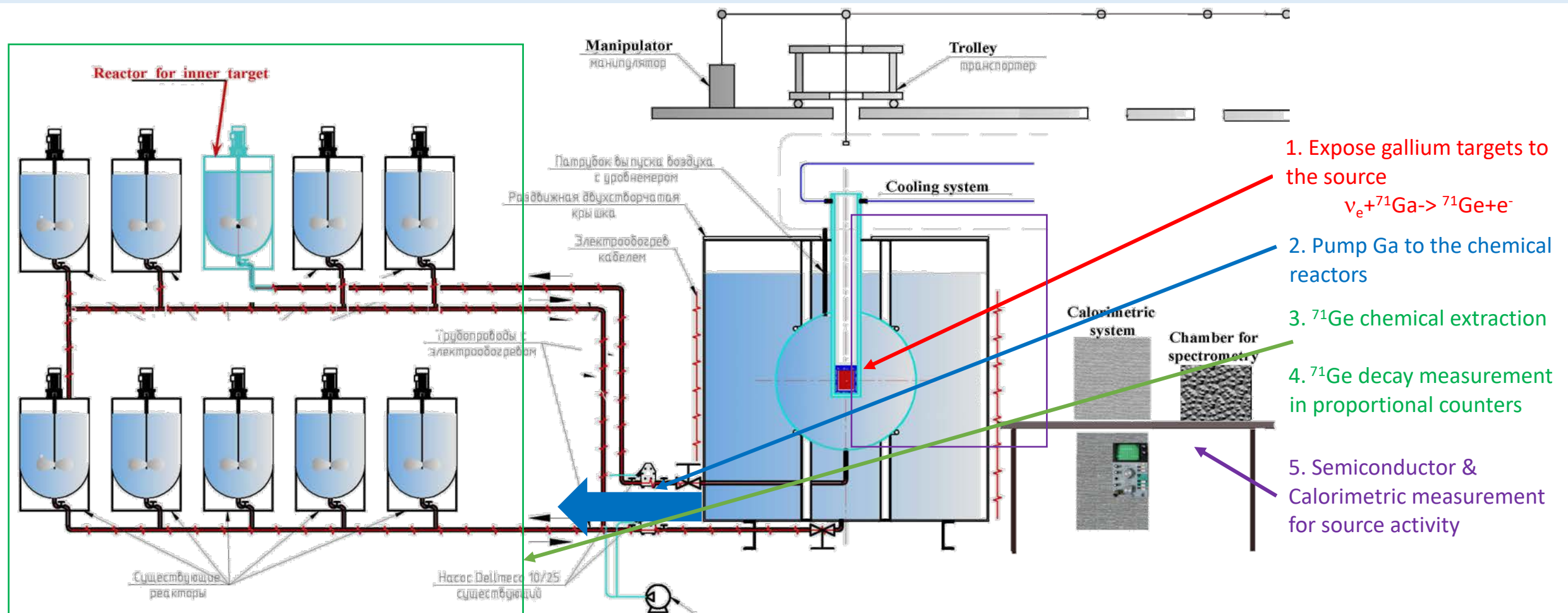
SAGE

Laboratory Photo showing extraction reactors

Global intensity of muon
$(3.03 \pm 0.19) \times 10^{-9}$ /(cm^{2}s)
Fast neutron flux (>3MeV)
$(6.28 \pm 2.20) \times 10^{-8}$ /(cm^{2}s)

Neutrino Source
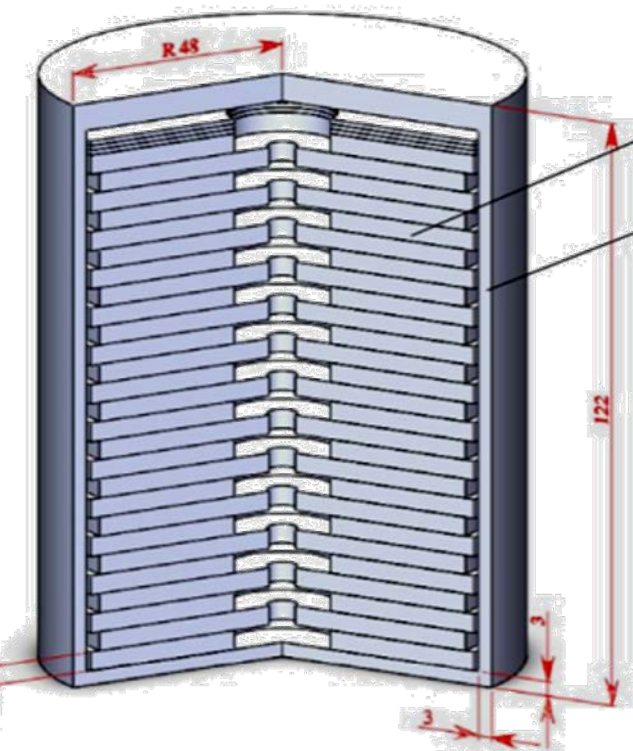
26 Cr disks

Stainless steel

Installed at the center of the two concentric zones

Irradiated for ~100 days with thermal neutrons in the SM-3 reactor (RIAR, Dmitrovgrad) to produce ^{51}Cr neutrino source

Thermal neutron flux density – 5×10^{15} n/(cm^2 s)

R 48

122

3

3

^{51}Cr (27.7 days)

427 keV ν (9.0%)
432 keV ν (0.9%)

747 keV ν (81.6%)
752 keV ν (8.5%)

320 keV γ

^{51}V (stable)

4 kg 97%-enriched ^{50}Cr,
26 chromium disks
h = 4 mm, $\varnothing$ 84 and 88 mm.

Simple and very well-understood neutrino spectrum

^{51}Cr Source (JINST 16 (2021) P04012)

Neutrino Source

Transport Container

Measurement Cell
Of Calorimeter

Ga Target
Containment

Activity at 14:02 on July 5, 2019
A = 3.414 ± 0.008 MCi
Energy/decay = 36.750 ± 0.84 keV

Flow
Meter

Temp.
Buffer

Circulation
thermostat

Pump

Measurement Cell

Cr
Source

Source Activity Measurements

lator
Trolley
Cooling system
Calorimetric system
Chamber for spectrometry
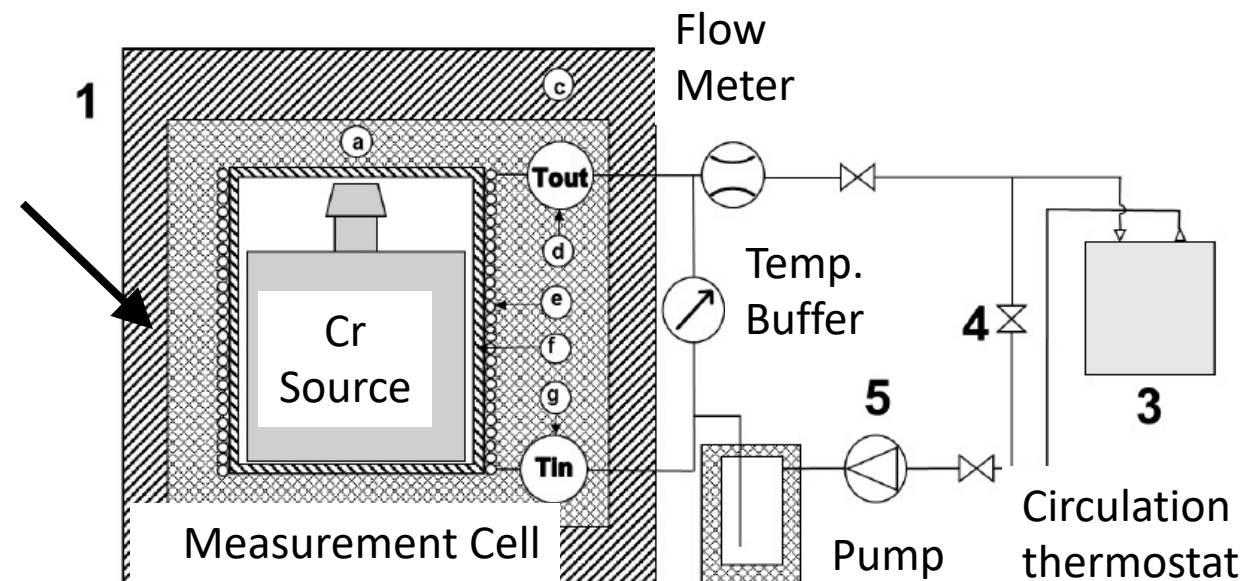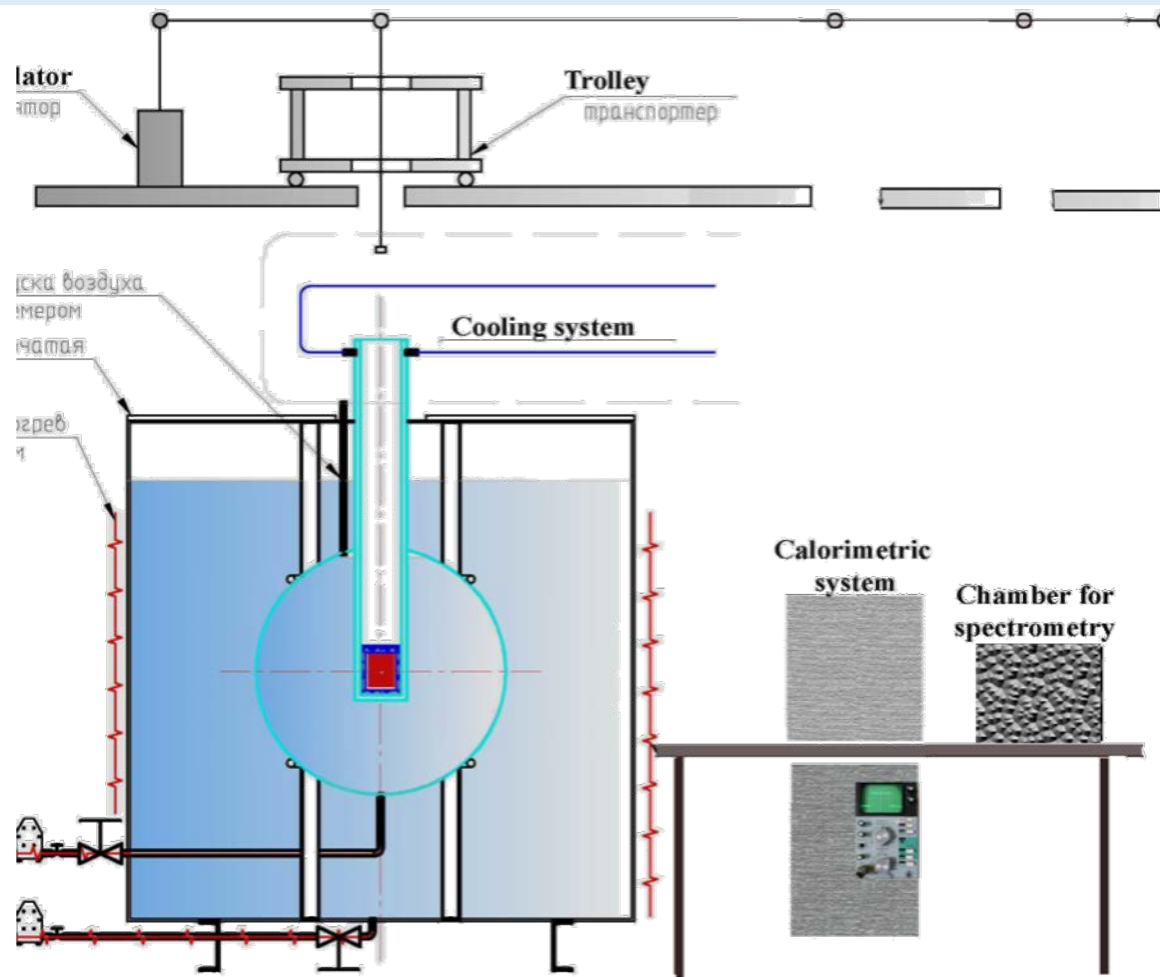
1) Move the source into a lead container
2) Measure γ spectrum at 21.65 m with a Ge detector *(1h)*
3) Move the source into the calorimeter
4) Measure the heat emitted by the source *(20-21 h)*

BEST Extraction Procedure (PRC 60 (1999) 055801)

^{71}Ge extraction (30 hours in *total*) :

1) Pump Ga from each zone to chemical reactors: inner zone → 1 reactor, outer zone → 6 reactors; *(4.5 h)*.

2) In each reactor the germanium carrier, in the form of GeCl$_4$, is extracted from the metal into aqueous phase by an oxidation reaction. DI H$_2$0, HCl and H$_2$O$_2$ are added and stirring forms the extraction solution.

3) The aqueous solution is concentrated by evaporation. *(16h)*

4) The gas GeH$_4$ is synthesized, mixed with Xe, and placed into a proportional counter.

5) ^{71}Ge decays are counted. *(60 – 150 days)*

Mixer motor

Ga level

Mixing vanes

Heaters
Stirrer

Teflon tank

Ga pumping system
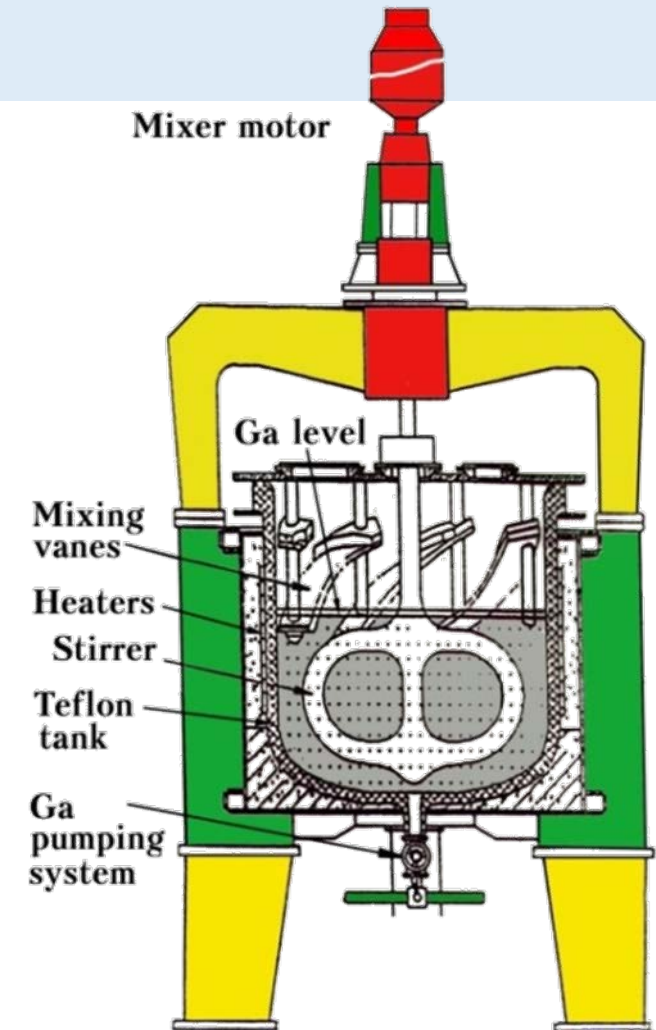
Extraction Efficiency of ^{71}Ge and Ge Carrier

Efficiency is measured by adding a known amount of (stable) Ge and measuring the mass of extracted Ge (Int. J. Mass Spec. 392 (2015) 41)

Amount of added Ge carriers (about 175 μg):

- 2.4 μmol ^{72}Ge (92%)

- 2.4 μmol ^{76}Ge (95%)

Mean extraction efficiency from Ga: 98%

Mean overall efficiency (including GeH$_4$ synthesis): 96%

Gas Synthesis Procedure (PRC 60 (1999) 055801)

- NaOH is added to concentrated aqueous solution to adjust pH.

- Air is swept out with a He flow.

- Low tritium $NaBH_4$ dissolved in H_2O is added.

- Mixture is heated.

- The Ge is reduced by $NaBH_4$ to make GeH_4.

- He sweeps the GeH_4 onto a chromatography column at -196^oC.

- When reaction complete, column is warmed and GeH_4 is eluted and captured.

- A measured quantity of old low-background Xe is added to make gas mixture.

Data Acquisition
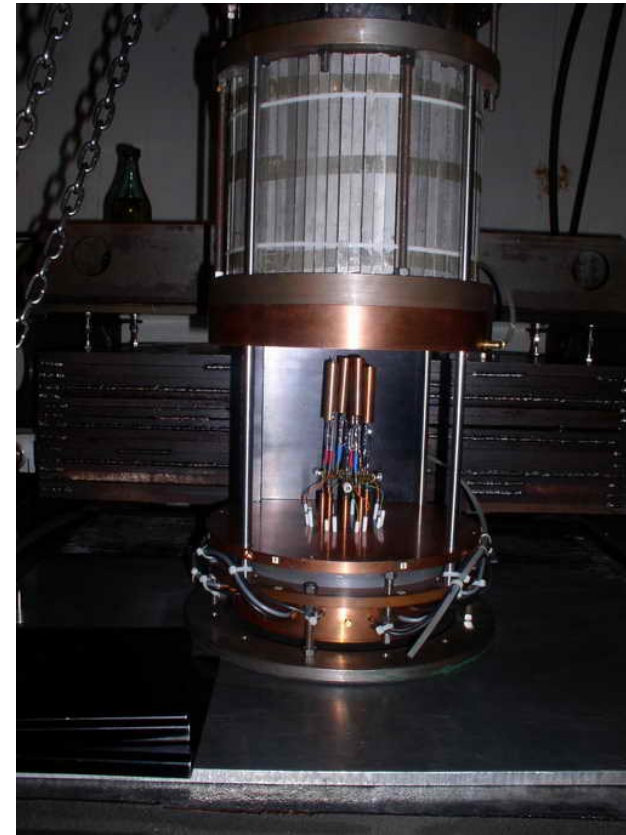
- Two 8-channel systems
- PC contained within NaI well
- PC pulses digitized at 1GHz, 100 MHz bandwidth, 8 bit
- Risetime = 3.5 ns
- 0.37<E<15 keV

^{71}Ge Decay

Auger decays produce point-like ionization in gas. In contrast β's or Compton recoils might deposit a similar amount of energy, but over an extended path.

Leads to a pulse shape analysis technique to remove them. BEST fits the pulse waveform.

ADP (Cl expt.): Astrophys. J. 496 (1998) 505
Pulse fit: NIM A290 (1990) 158

- Half-life of 11.43 d, ground state transition

- K Capture (88% of all decays)
  - 41.5% Auger e- 10.367 keV
  - 41.2% Auger e- 1.2 keV & x ray 9.2 keV
  - 5.3% Auger e- 0.12 keV & x ray 10.26 keV

- L and M capture give almost entirely Auger e-
  - L gives 1.2 keV Auger, M gives 0.12 keV Auger

- The proportional counter observes Auger e- with high efficiency
  - The X ray efficiency is much less
  - As a result, the number of K/L peak counts are about equal

^{71}Ge Candidate Event Selection

- Energy calibration

- Time tagging
  - Periods of expected high background
    - Reject 2.6-hour periods after shield opening, to eliminate Rn induced backgrounds (~1.2% of the total run time)
  - Anti-coincidence with NaI system (1/3 of events removed)

- Pulse shape analysis
  - Alpha-induced events
  - High-voltage breakdowns
  - Compton scattering
  - Beta-induced backgrounds

~1.5 evts /day

Risetime (RT) of the pulses

Days 0 – 30

Days 40-70
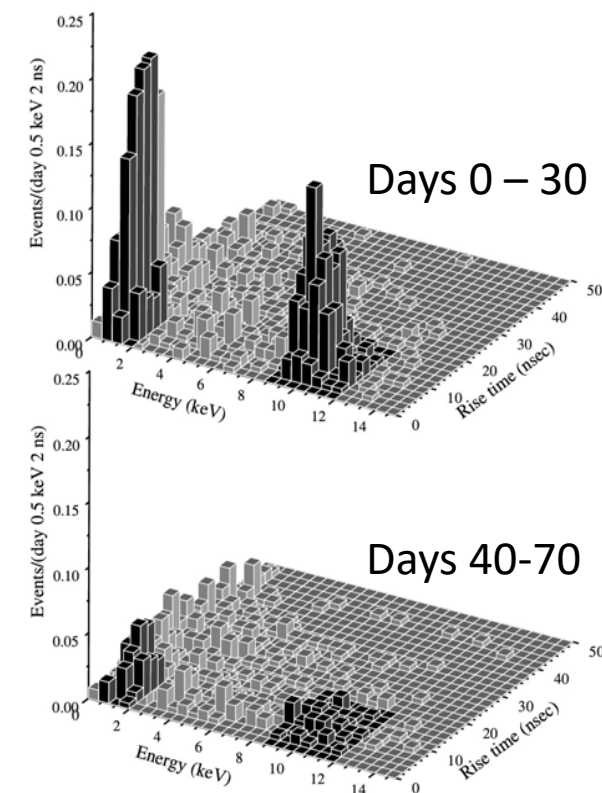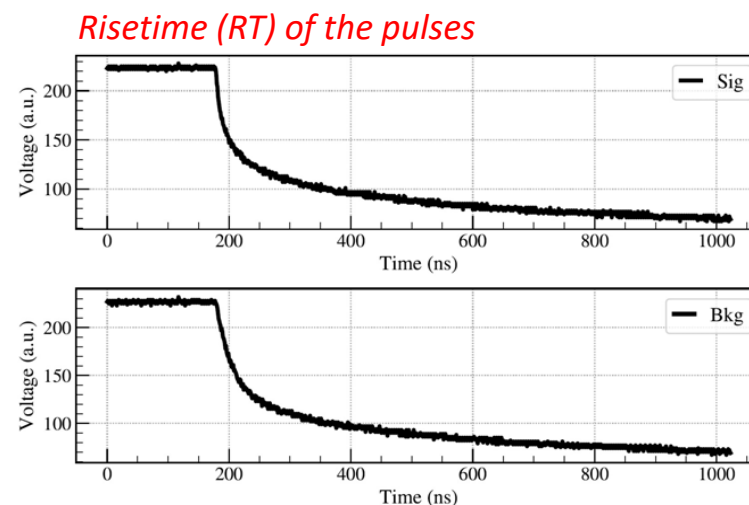
Energy Calibration

PRC **60**, (1999) 055801

$$\frac{P_K(^{71}\text{Ge})}{P(^{55}\text{Fe})} = \frac{10.367}{5.895}[1 - (4.5G + 2.78)(V - V_{\text{crit1}}) \times 10^{-6}] ,$$

$$\frac{R_K(^{71}\text{Ge})}{R(^{55}\text{Fe})} = \sqrt{\frac{5.895}{10.367}}[1 + 1.5 \times 10^{-3}(V - V_{\text{crit2}})] ,$$

$$V_{\text{crit1}} = 10.5G + 0.6P + 588 \quad V_{\text{crit2}} = 6G + P/3 + 824$$

| Counter	^{55}Fe Pos. (a.u.)	^{55}Fe Resol. (%)	En non-linearity factor	L-peak Position Pred. from ^{55}Fe	L-peak Position True	L-peak Position Ratio	L-peak Resolution Pred. from ^{55}Fe	L-peak Resolution True	L-peak Resolution Ratio	K-peak Position Pred. from ^{55}Fe	K-peak Position True	K-peak Position Ratio	K-peak Resolution Pred. from ^{55}Fe	K-peak Resolution True	K-peak Resolution Ratio
sys2z															
YCN43	437.39	18.2	0.982	86.81	87.16	1.00	40.92	40.29	0.98	755.35	725.50	0.96	15.88	12.98	0.82
YCNA9	431.86	19.7	0.938	85.71	86.32	1.01	44.29	42.57	0.96	712.39	728.84	1.02	17.19	16.02	0.93
YCN41	442.80	18.0	0.967	87.88	87.00	0.99	40.40	37.24	0.92	753.01	732.49	0.97	15.68	13.34	0.85
YCN46	448.93	18.5	0.915	89.10	90.61	1.02	41.48	39.62	1.04	722.39	748.55	0.96	16.10	14.16	0.88
Mean sys2z						1.00			0.96			1.00			0.87
std						0.01			0.03			0.04			0.05
sys3															
YCN113	337.36	18.8	0.982	66.96	57.71	0.86	42.09	42.13	1.00	582.61	564.38	0.97	16.34	14.13	0.86
YCT92	334.67	18.9	0.964	66.42	56.72	0.85	42.40	41.88	0.99	567.37	563.97	0.99	16.46	13.90	0.84
YCT3	342.65	19.3	0.932	68.01	58.24	0.86	43.23	40.61	0.94	561.61	576.97	1.03	16.78	14.19	0.85
YCT2	337.00	18.8	0.982	66.89	57.77	0.86	42.24	41.62	0.99	581.98	563.33	0.97	16.40	14.05	0.86
YCT9	334.80	19.1	0.978	66.45	57.97	0.87	42.90	39.42	0.92	575.83	569.62	0.99	16.65	13.89	0.83
YCT97	332.81	18.6	0.932	66.05	57.11	0.86	41.64	38.75	0.93	545.48	559.25	1.03	16.16	13.51	0.84
Mean sys3						0.86			0.96			1.00			0.85
std						0.01			0.03			0.03			0.01

- Bi-weekly calibration with ^{55}Fe source, 5.9 keV.
- Calibration gain and resolution scaled to K/L peaks using an empirical formula adjusting for GeH_4 fraction (G) and pressure (P).
- Energy Selection 98.1% ($\pm$1 FWHM) acceptance for K and L peaks.
- Peak position & resolution verified by separate ^{71}Ge measurements.

Pulse Shape Analysis

- Exclude Flat-top waveforms (~1.5 events/day)
  - Alpha-induced events
  - High-voltage breakdowns

- Fit rise-time (T_N) to pulses with extended ionization formulism
  - Compton scattering
  - Beta-induced backgrounds

Days 0 − 30

Days 40-70

Slower fall-time
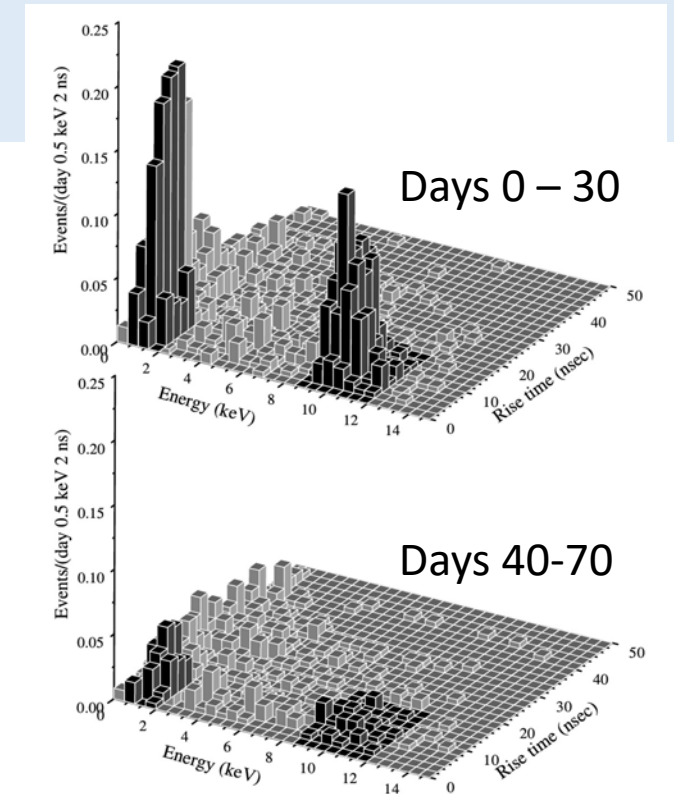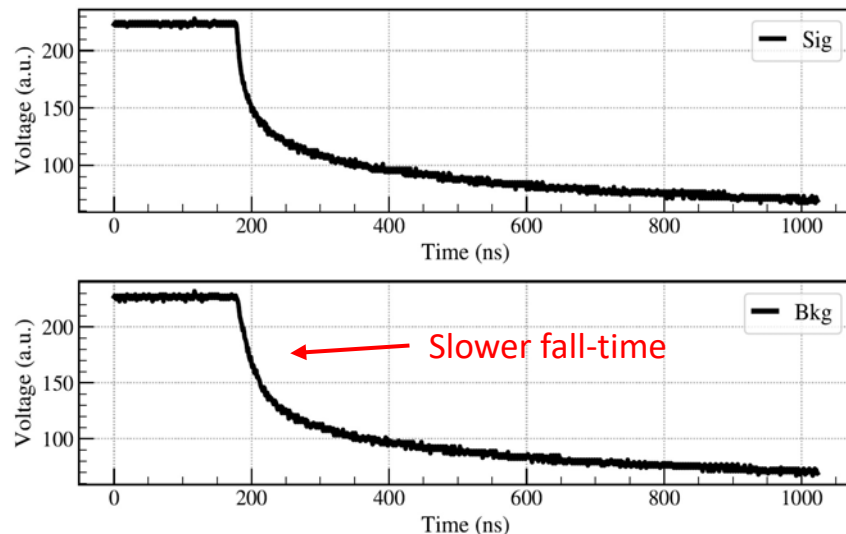
$$V(0 < t < T_N) = V_0 \left[\frac{t + t_0}{T_N} \ln\left(1 + \frac{t}{t_0}\right) - \frac{t}{T_N} \right],$$

$$V(t > T_N) = V_0 \left[\ln\left(1 + \frac{t - T_N}{t_0}\right) - 1 - \frac{t + t_0}{T_N} \ln\left(1 - \frac{T_N}{t + t_0}\right) \right]$$

NIM A290 (1990) 158

Pulse Shape Analysis

- The rise time cut values were measured for each counter used in the experiment.
  - A trace of active $^{71}GeH_4$ was added to each counter to determine its T_N.
  - Counters filled with typical gas mixture. Efficiency accounts for pressure and GeH_4 fraction.
  - 96% acceptance window for each detector was determined (limit on T_N).

Counter Filling					T_N	
Extraction name	Counter name	Pressure (mmHg)	GeH4 fraction (%)	Syst. Slot	K-peak	L-peak
Inner-1	YCT92	630	8.8	3.5	17.6	13.0
Inner-2	YCT2	640	9.5	3.2	16.6	10.1
Inner-3	YCN43	650	9.3	Z.3	13.2	10.0
Inner-4	YCT97	640	9.2	3.7	17.3	11.4
Inner-5	YCN46	650	9.5	Z.8	15.2	11.3
Inner-6	YCN42	640	9.8	3.8	13.2	9.1
Inner-7	YCT92	640	9.3	3.5	17.6	13.0
Inner-8	YCT2	645	9.5	3.2	16.6	10.1
Inner-9	YCN43	640	9.1	Z.3	13.2	10.0
Inner-10	YCT97	650	9.1	3.7	17.3	11.4

Counter Filling					T_N	
Extraction name	Counter name	Pressure (mmHg)	GeH4 fraction (%)	Syst. Slot	K-peak	L-peak
Outer-1	YCN113	635	9.5	3.4	13.6	9.1
Outer-2	YCT3	635	9.5	3.1	16.4	10.3
Outer-3	YCNA9	640	10.5	Z.4	18.8	13.2
Outer-4	YCT9	635	9.6	3.6	14.9	9.1
Outer-5	YCN41	635	10.0	Z.1	13.4	10.3
Outer-6	YCT4	630	9.0	3.3	13.2	10.2
Outer-7	YCN113	630	10.3	3.4	13.6	9.1
Outer-8	YCT3	640	9.5	3.1	16.4	10.3
Outer-9	YCNA9	635	9.9	Z.4	18.8	13.2
Outer-10	YCT9	645	9.5	3.6	14.9	9.1

Likelihood Fit

- Maximum likelihood fit to the *t* and *E* dependence of each candidate event

$$\mathcal{L} = e^{-p\epsilon\Delta/\lambda - b\tau} \prod_{i}^{l} \left[\frac{w_p(E_i)}{w_b(E_i)} p\epsilon e^{-\lambda t_i} + b \right]$$

(PRC 60, 055801 (1999))

p: ^{71}Ge production rate, 11.4-d half-life
b: background rate, constant in time
ε: overall efficiency
$w_p(E)$ /$w_b(E)$: energy weight factors
Δ: probability an event will during counting
τ : total counting time

* Weight factors are determined by examining the energy spectra for each counter

Example Fit
Third Extraction from Inner Volume

data cummulative, delta: 0.774, Live Time: 50.52
signal: 55.79, background: 10.21

Counting Results

Production rates for the inner target

Production rates for the outer Target

Inner Zone
Blue=predicted
Red=measured

Outer Zone

Predicted Production Rates

$$\nu_e + {}^{71}\text{Ga} \rightarrow {}^{71}\text{Ge} + e^-$$
$${}^{71}\text{Ge} + e^- \rightarrow {}^{71}\text{Ga} + \nu_e$$

Production rates are predicted from cross section
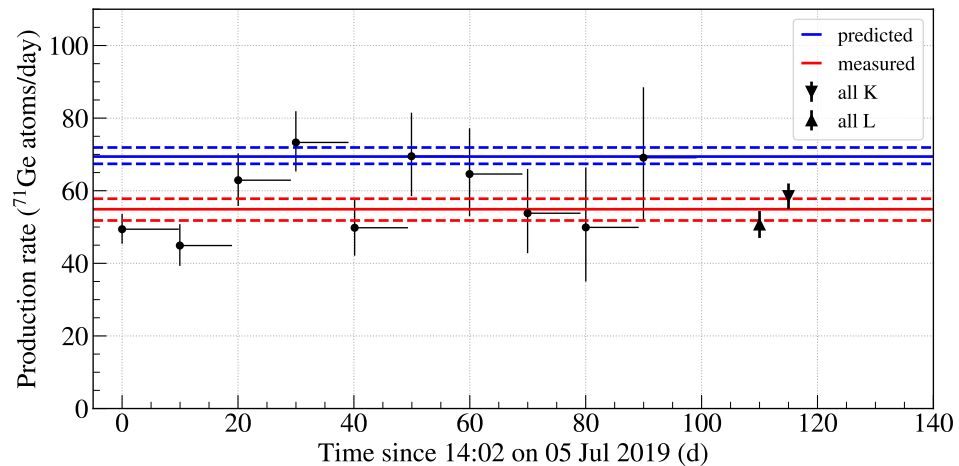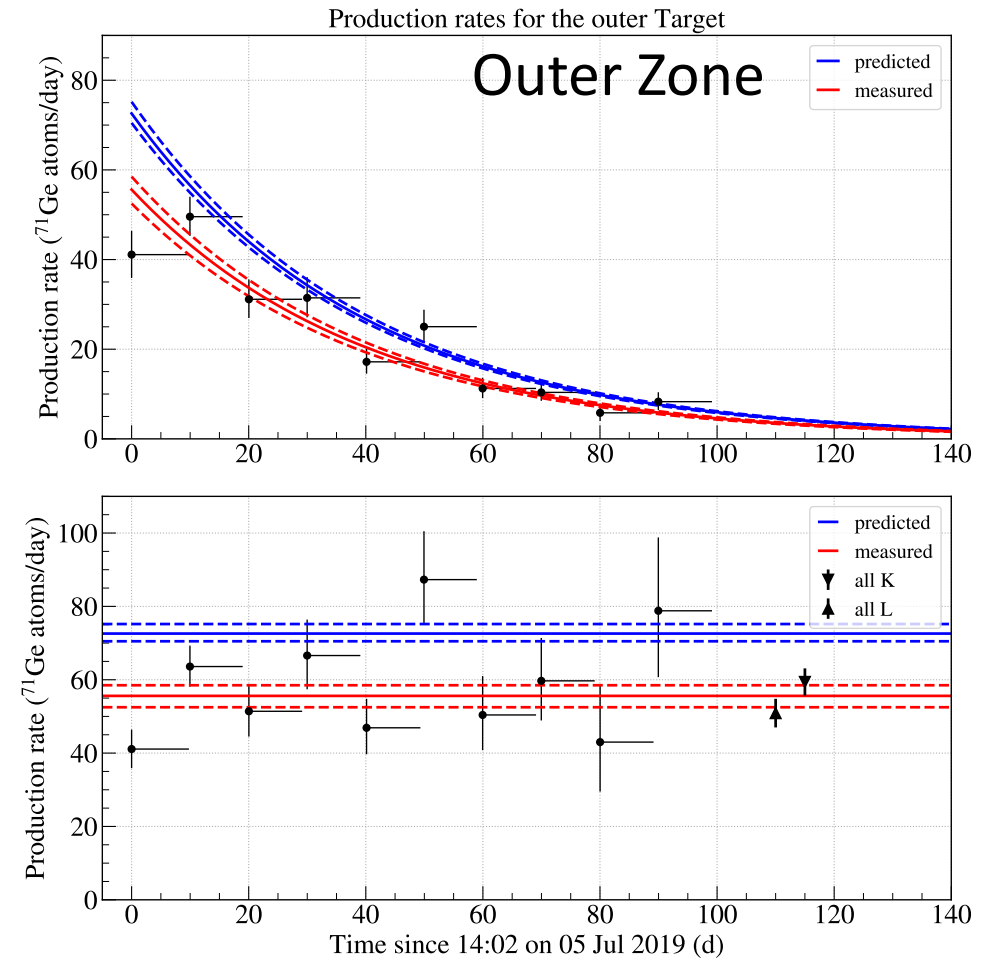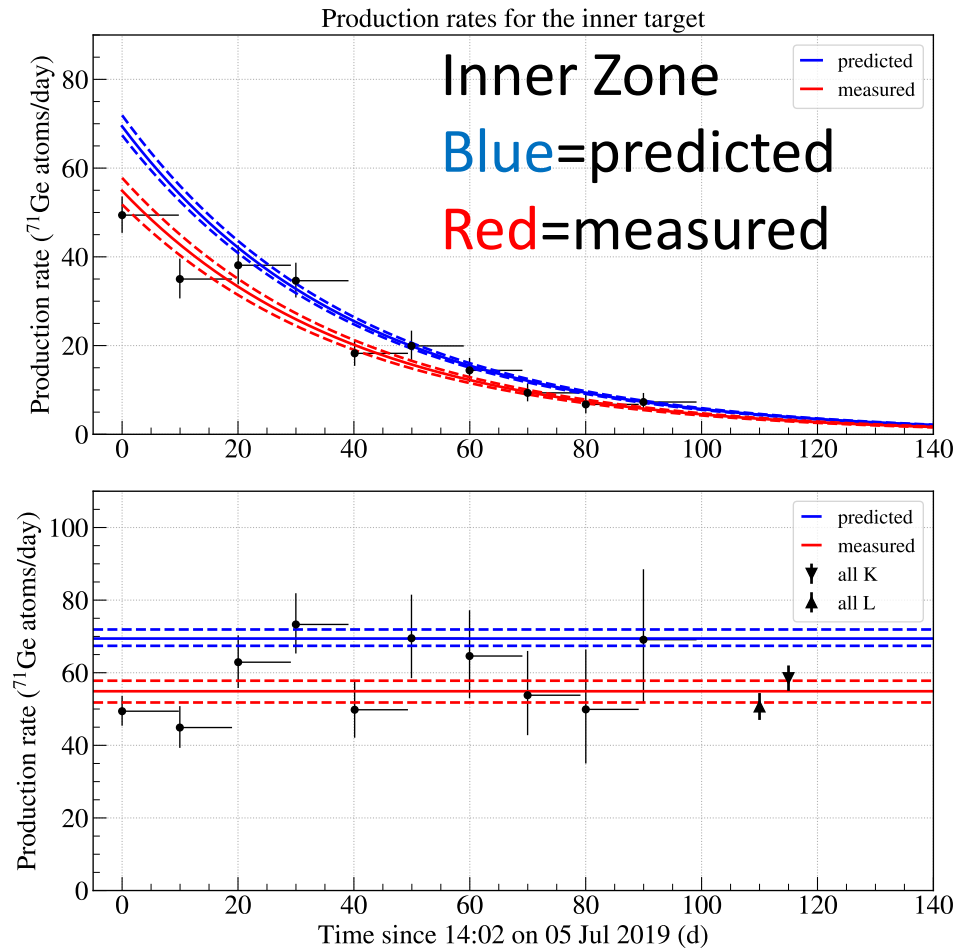
$$P_{ee}(E_\nu, r) = 1 - \sin^2 2\theta \sin^2 \left(1.27 \frac{\Delta m^2 [\text{eV}^2] r [\text{m}]}{E_\nu [\text{MeV}]} \right)$$

$$R_j = \frac{n\sigma A}{4\pi} \int_{V_j} \frac{P_{ee}(r)}{r^2} d\vec{x} \approx V_0 \frac{1}{N} \sum_{i=1}^{N} \frac{P_{ee}(r)}{r^2} \Theta_j(\vec{x}_i)$$

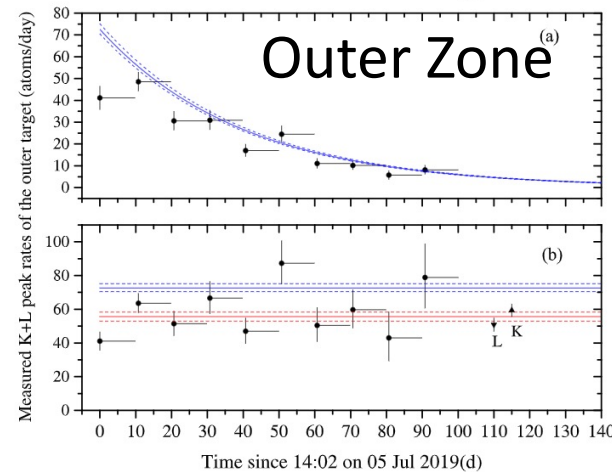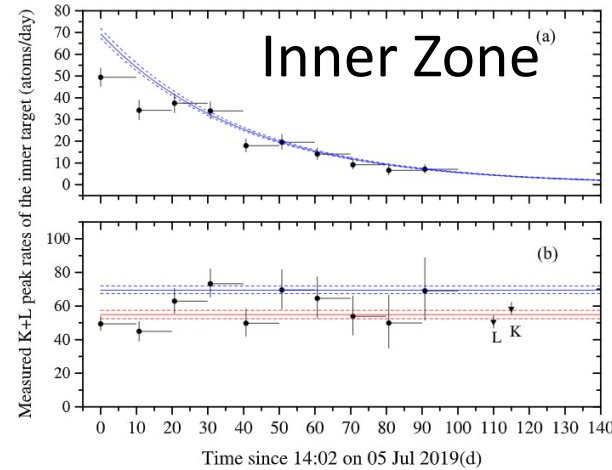|	Value	Uncertainty	
		Magnitude	%
Atomic density $D = \rho N_0 f_1 / M$			
Ga density ρ (g Ga/cm^3)	6.095	0.002	0.033
Avogadro's number N_0 (10^{23} atoms Ga/mol)	6.0221	0.0	0.0
Ga molecular weight M (g Ga/mol)	69.72307	0.00013	0.0002
Atomic density D (10^{22} atoms ^{71}Ga/cm^3)	2.1001	0.0008	0.037
Source activity at reference time A, MCi	3.414	0.008	0.23
Cross section σ (10^{45} cm^2/ (^{71}Ga atom ^{51}Cr decay)], Bahcall	5.81	+0.21,-0.16	+3.6,-2.8
Path length in Ga $< L_{in} >$ (cm)	52.03	0.18	0.3
Path length in Ga $< L_{out} >$ (cm)	54.41	0.18	0.3
Predicted production rate (^{71}Ge atoms/d), R_{In}	69.41	+2.5,-2.0	+3.6,-2.8
Predicted production rate (^{71}Ge atoms/d), R_{Out}	72.59	+2.6,-2.1	+3.6,-2.8

Predicted vs. Measured Production Rates

K+L-peak

Extraction	Number of candidate events	Number fit to ^{71}Ge	^{51}Cr source production	Solar ν production	Carryover	^{71}Ge Production decay rate (atoms/day)
Inner-1	180	176.3	175.5	0.8	0.0	$49.4^{+4.0}_{-4.2}$
Inner-2	129	111.5	107.7	0.8	3.1	$44.9^{+5.6}_{-5.9}$
Inner-3	132	117.6	115.3	0.7	1.6	$62.9^{+7.1}_{-7.4}$
Inner-4	93	87.3	85.6	0.6	1.1	$73.3^{+8.0}_{-8.6}$
Inner-5	134	60.2	58.4	0.6	1.2	$49.8^{+7.7}_{-8.2}$
Inner-6	81	48.8	47.7	0.4	0.7	$69.5^{+11.0}_{-12.0}$
Inner-7	91	45.0	43.9	0.5	0.6	$64.6^{+11.6}_{-12.6}$
Inner-8	59	33.6	32.4	0.6	0.6	$53.8^{+11.0}_{-12.2}$
Inner-9	106	23.7	22.7	0.6	0.4	$49.9^{+14.9}_{-16.5}$
Inner-10	88	25.2	24.3	0.6	0.3	$69.1^{+17.3}_{-19.4}$
Comb. K+L	1093	724.0	708.2	6.1	9.7	$54.9^{+2.4}_{-2.5}$

K+L-peak

Extraction	Number of candidate events	Number fit to ^{71}Ge	^{51}Cr source production	Solar ν production	Carryover	^{71}Ge Production decay rate (atoms/day)
Outer-1	181	133.4	129.6	3.7	0.1	$41.1^{+5.2}_{-5.3}$
Outer-2	174	163.8	158.6	3.3	1.9	$63.6^{+5.5}_{-5.7}$
Outer-3	116	92.5	88.2	2.8	1.5	$51.4^{+6.9}_{-7.3}$
Outer-4	98	82.3	78.9	2.5	0.8	$66.6^{+9.2}_{-9.8}$
Outer-5	120	64.0	59.5	3.5	1.0	$46.9^{+7.2}_{-7.9}$
Outer-6	97	62.3	59.3	2.6	0.4	$87.3^{+12.3}_{-13.2}$
Outer-7	69	38.0	34.4	3.2	0.4	$50.4^{+9.6}_{-10.6}$
Outer-8	68	43.4	39.2	3.9	0.4	$59.7^{+10.8}_{-11.7}$
Outer-9	66	20.2	17.0	3.0	0.2	$43.0^{+13.5}_{-15.3}$
Outer-10	81	31.8	28.0	3.6	0.2	$78.8^{+18.1}_{-20.0}$
Comb. K+L	1069	738.8	699.8	32.2	6.8	$55.6^{+2.6}_{-2.7}$

Inner Zone

Outer Zone

	IN	OUT
Predicted	$69.41^{+2.5}_{-2.0}$	$72.59^{+2.6}_{-2.1}$
Measured	54.9 ± 2.9	55.6 ± 3.1
Ratio	0.79 ± 0.05	0.77 ± 0.05

4.2σ and 4.8σ less than the unity

$$\text{Note: } \frac{0.77 \pm 0.05}{0.79 \pm 0.05} = 0.97 \pm 0.07$$

Similar deficits observed in both zones

Oscillation Interpretation

Exclusion curves are calculated by a global minimization of χ^2:

$$\chi^2(\Delta m^2, \sin^2 2\theta) = \left(R^{\text{meas.}} - R^{\text{calc.}}\right)^{\text{T}} V^{-1}\left(R^{\text{meas.}} - R^{\text{calc.}}\right)$$

$R^{\text{meas.}}$: vector of measured rates
$R^{\text{calc.}}$: vector of calculated rates with
$R_i^{\text{calc.}}(\Delta m^2, \sin^2 2\theta)$
V: covariance matrix

❖ For the Ga source experiments, the cross section uncertainties are the only significant contribution to the correlated uncertainty.
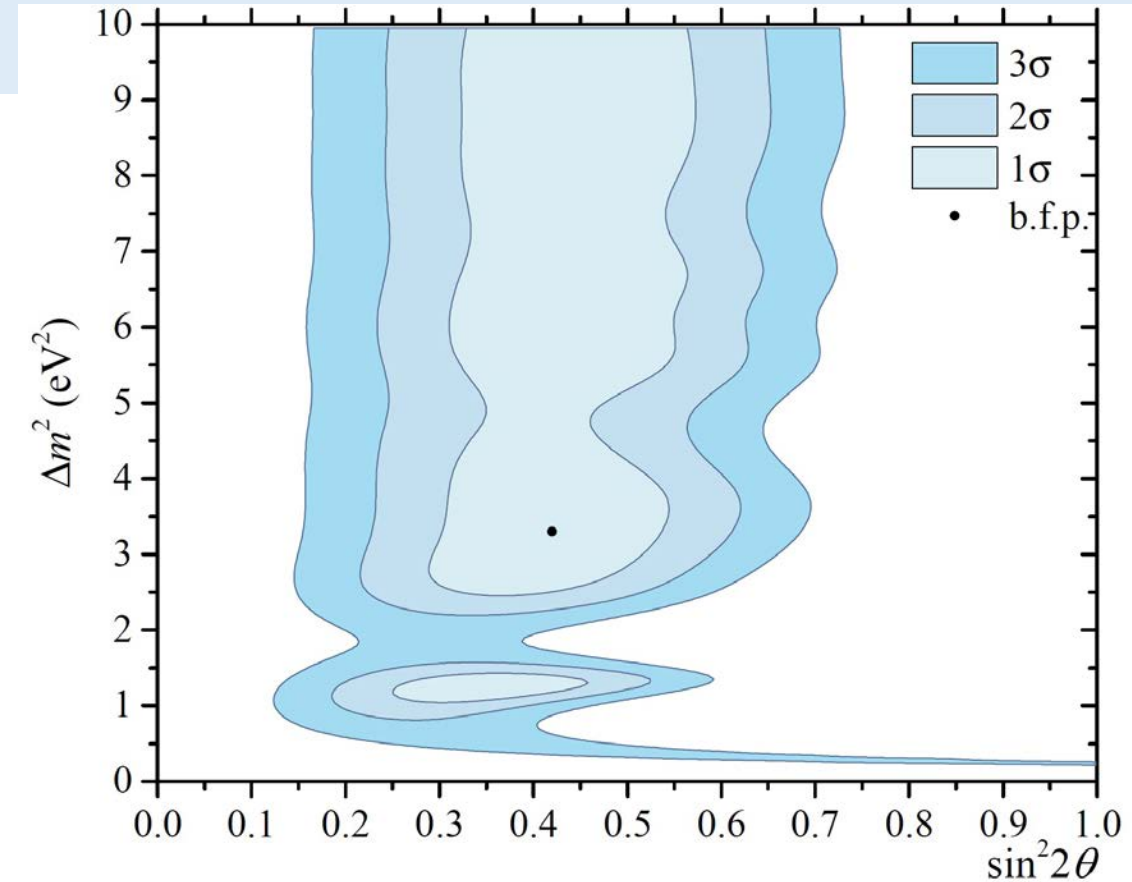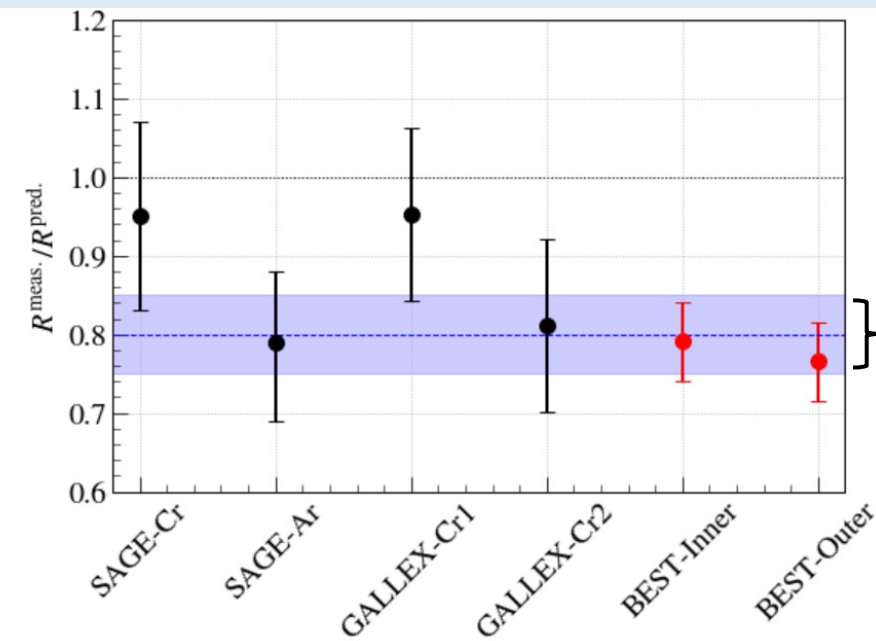

FIG. 7. Allowed regions for two BEST results. The best-fit point is $\sin^2 2\theta = 0.42$, $\Delta m^2 = 3.3$ eV^2 and is indicated by a point.

Combined Analysis with Other Ga Source Experiments

Combined result:
$$R_0 = 0.80 \pm 0.05$$

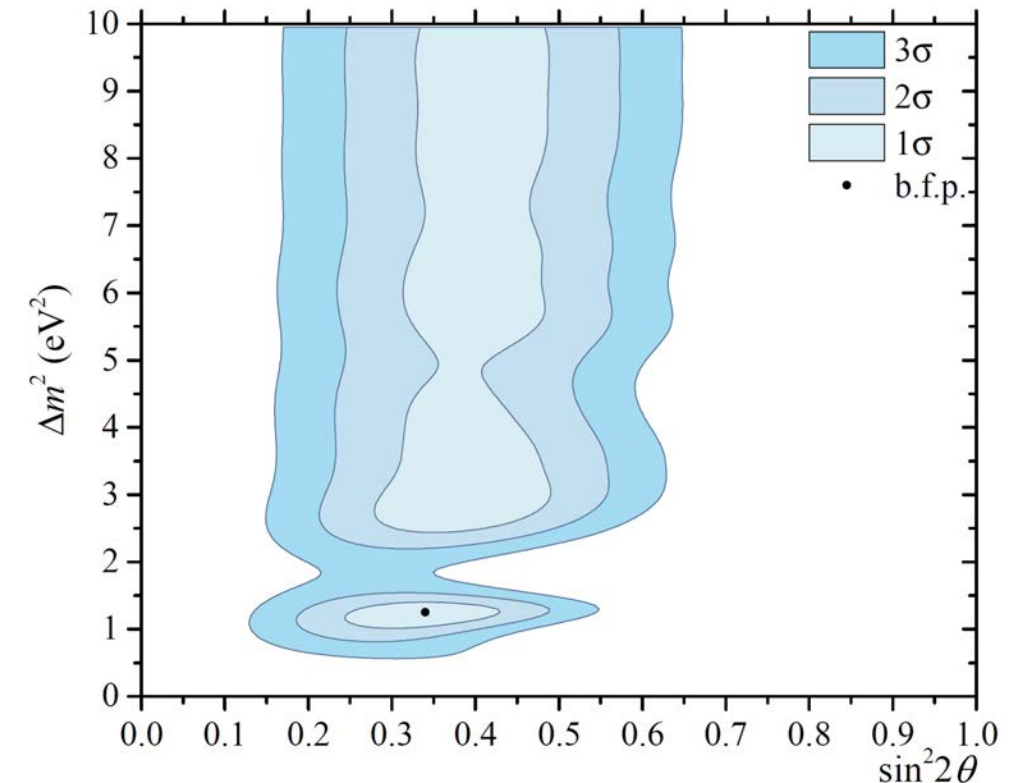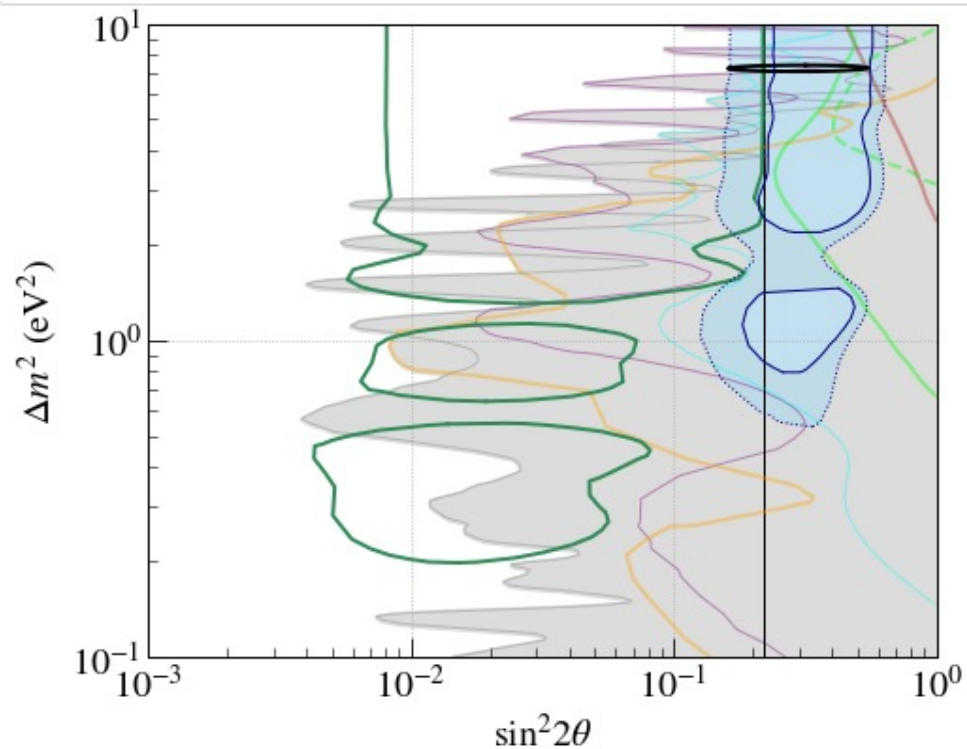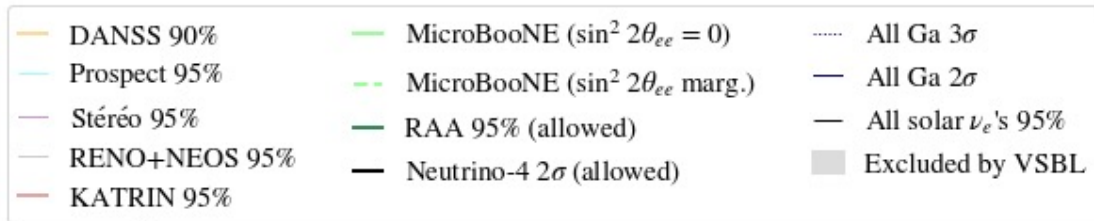| Experiment	Measured/Predicted	Ref.
SAGE-Cr	0.95 ± 0.12	PRC **59**, 2246 (1999)
SAGE-Ar	$0.79^{+0.09}_{-0.10}$	PRC **73**, 045805 (2006)
GALLEX-Cr1	0.95 ± 0.11	PLB **420**, 114 (1998)
GALLEX-Cr1	0.81 ± 0.11	PLB **420**, 114 (1998)
BEST-Inner	0.791 ± 0.05	arXiv:2109.11482
BEST-Inner	0.766 ± 0.05	arXiv:2109.11482

FIG. 8. Allowed regions for two GALLEX, two SAGE and two BEST results. The best-fit point is $\sin^2 2\theta = 0.33$, $\Delta m^2 = 1.25$ eV^2 and is indicated by a point.

Comparison to Other Oscillation Results

DANSS 90%
Prospect 95%
Stéréo 95%
RENO+NEOS 95%
KATRIN 95%
MicroBooNE ($\sin^2 2\theta_{ee} = 0$)
MicroBooNE ($\sin^2 2\theta_{ee}$ marg.)
RAA 95% (allowed)
Neutrino-4 2σ (allowed)
All Ga 3σ
All Ga 2σ
All solar ν_e's 95%
Excluded by VSBL

Clear tension between the numerous results.

BEST Best-fit point
$\Delta m^2 = 1.25$
$\sin^2 2\theta = 0.34$

DANSS: Int. J. Mod. Phys. A **35**, 2044015 (2020)
Prospect: PRD **103**,032001 (2021)
Stereo: PRD **102**, 052002 (2020)
RENO+NEOS: arXiv:2011.00896 (2020)
KATRIN: PRL **126**, 091803 (2021)
MicroBooNE: arXiv:2111.10359
RAA: PRD **83**, 073006 (2011)
Neutrino-4: JETP Lett. **112**, 199 (2020)
Model indep. solar: PLB **816**, 136214 (2021)

Consistent with, but not Proof of, Oscillations

These results reaffirm the Ga anomaly, with higher statistical precision.
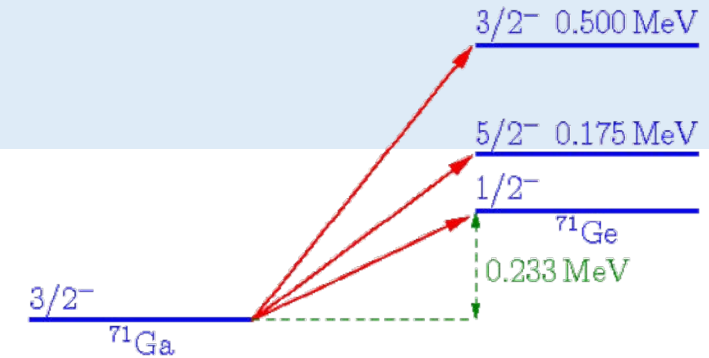
But no dependence on oscillation length was observed. So although the results are consistent with oscillations, there is no 'smoking gun' evidence that is not subject to caveats.

Because the rate in the two volumes is equally depressed, a number of potential explanations beyond oscillations have been considered. No clear alternative has been identified.
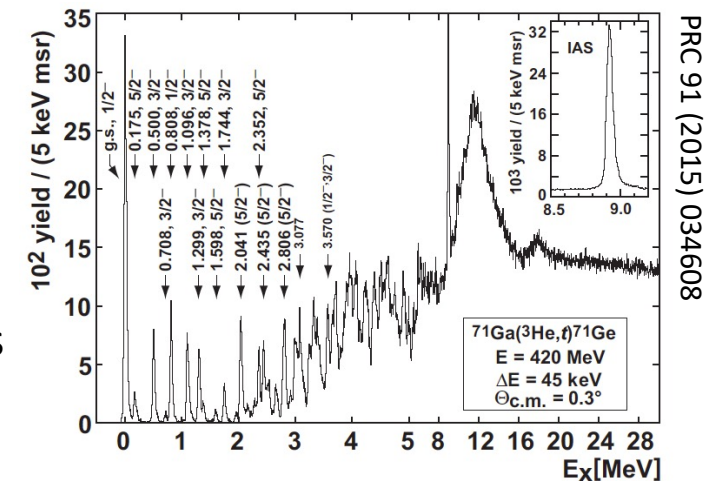
- Cross Section
- Source Strength
- Extraction Efficiencies
- Counting Efficiencies
- Average Path Length

The Cross Section

- Bahcall estimated the ground state cross section by deriving the transition strength from the well-known ^{71}Ge decay rate. (PRC 56 (1997) 3391)
    - The excited states (ES) were estimated from imprecise charge exchange measurements and found to be ~5%.

^{51}Cr and ^{37}Ar ν's can only excite first 3 levels in ^{71}Ge.

- Recently much better charge exchange measurements have become available. (PLB 706 (2011) 134, PLB 722 (2013) 233, PRC 91 (2015) 034608)
    - Show that the ES contribution is about 7%.
    - But, the Gamow-Teller and tensor contributions might cancel. (PLB 431 (1998) 110)

- New shell model calculations avoid the GT-tensor concern, but must reproduce other low energy characteristics. (PLB 795 (2019) 542)
    - This agreement is modest and not fully reassuring.
    - New shell model work is desirable.

- Bahcall's result is at the average of the two methods with an uncertainty that encompasses both, so BEST uses that value. 5.81x10^{-45} cm^2
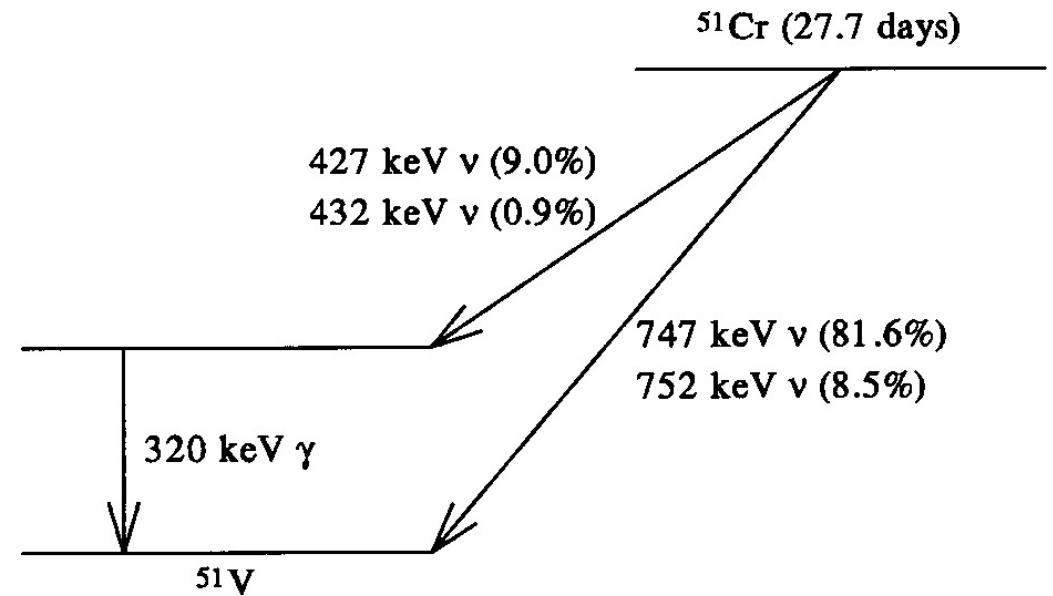
Source Strength

- The activity measurement precision is best from calorimetry.
- This technique has been confirmed by other estimates building confidence. (PRC 59 (1999) 2246)
  - Direct counting of 320-keV line with Ge detector.
  - Reactor physics and neutron transport.
- Cr decay scheme.
  - The branching ratio to the 320-keV level is key for interpreting the activity of the source.
  - It is claimed to be known to ~0.1%, too small to explain 20% depression.

^{51}Cr (27.7 days)

427 keV ν (9.0%)
432 keV ν (0.9%)

747 keV ν (81.6%)
752 keV ν (8.5%)

320 keV γ

^{51}V

SAGE Extraction Efficiencies (PRC 73 (2006) 045805)

- A variety of extraction efficiency tests have been done – all consistent with experimental values. (PRC 60 (1999) 055801)

- ^{70,72}Ga radioactive isotopes produced by neutron activation were used for the carrier. Extraction of the Ge isotopes resulting from their decay was as expected. Tests question that atomic excitations during nuclear processes result in Ge ending up in un-extractable chemical form.

- ^{68}Ge produced cosmogenically when the Ga resided on surface was counted during many initial extractions. The reduction during these extractions followed the expected trend.

- A sample of carrier doped with ^{71}Ge was produced and the measured extraction efficiency was as expected from the stable carrier determination.

Counting Efficiencies (PRC 60 (1999) 055801)

- Counter efficiencies were cross checked several ways.

- Volume efficiency checked with ^{37}Ar loaded counter gas
  - ^{40}Ca(n,a)^{37}Ar
  - Gas activity measured in a large counter (2.5 cm^3) with high efficiency
  - Then used in experiment's counters to determine efficiency

- L- & K-Peak Efficiencies with ^{69}Ge and ^{71}Ge loaded counter gas
  - ^{69}Ga(p,n)^{69}Ge
  - ^{69}GeH$_4$-Xe fill, measure Auger e$^-$ and 1106 γ ray. The relative rates of γ/e determines efficiency.
  - ^{70}Ge(n,g)^{71}Ge
  - ^{71}GeH$_4$-Xe fill, measure in both large and experimental counters

Window

Cathode

Gas fill tube

Anode
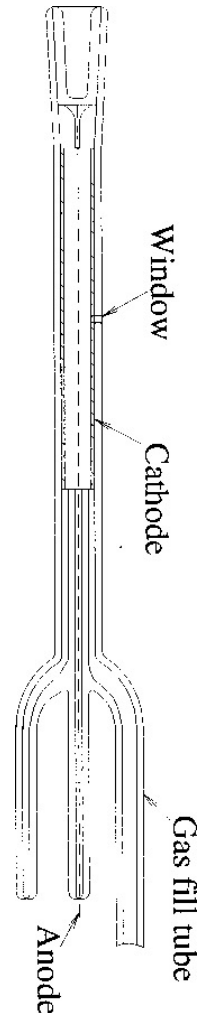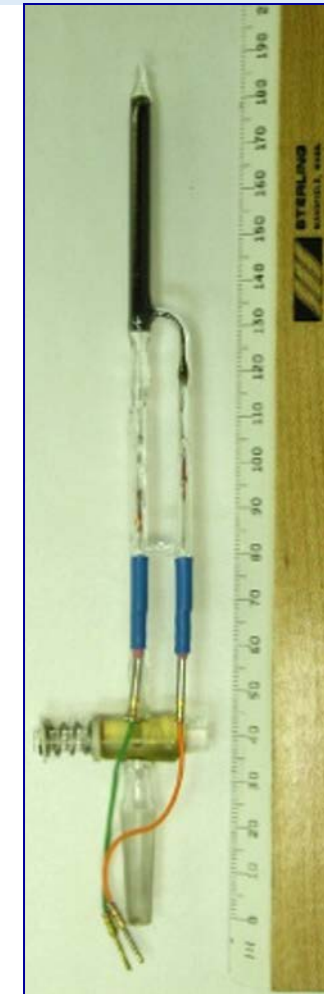
Average Path Length and Geometry

$$R_j = \frac{n\sigma A}{4\pi} \int_{V_j} \frac{P_{ee}(r)}{r^2} d\vec{x} \approx V_0 \frac{1}{N} \sum_{i=1}^{N} \frac{P_{ee}(r)}{r^2} \Theta_j(\vec{x}_i)$$

Due to irregular geometry, calculated by Monte Carlo Integration.
Verified by comparing calculated Ga masses to measured.
Uncertainty estimated by varying geometry parameters.
Uncertainty about 0.3%.

$<L_{in}>$ = 52.03 ± 0.18 cm
$<L_{out}>$ = 54.41 ± 0.18 cm

These are the average path length of a neutrino through the Ga zone. It is <u>not</u> the oscillation length.
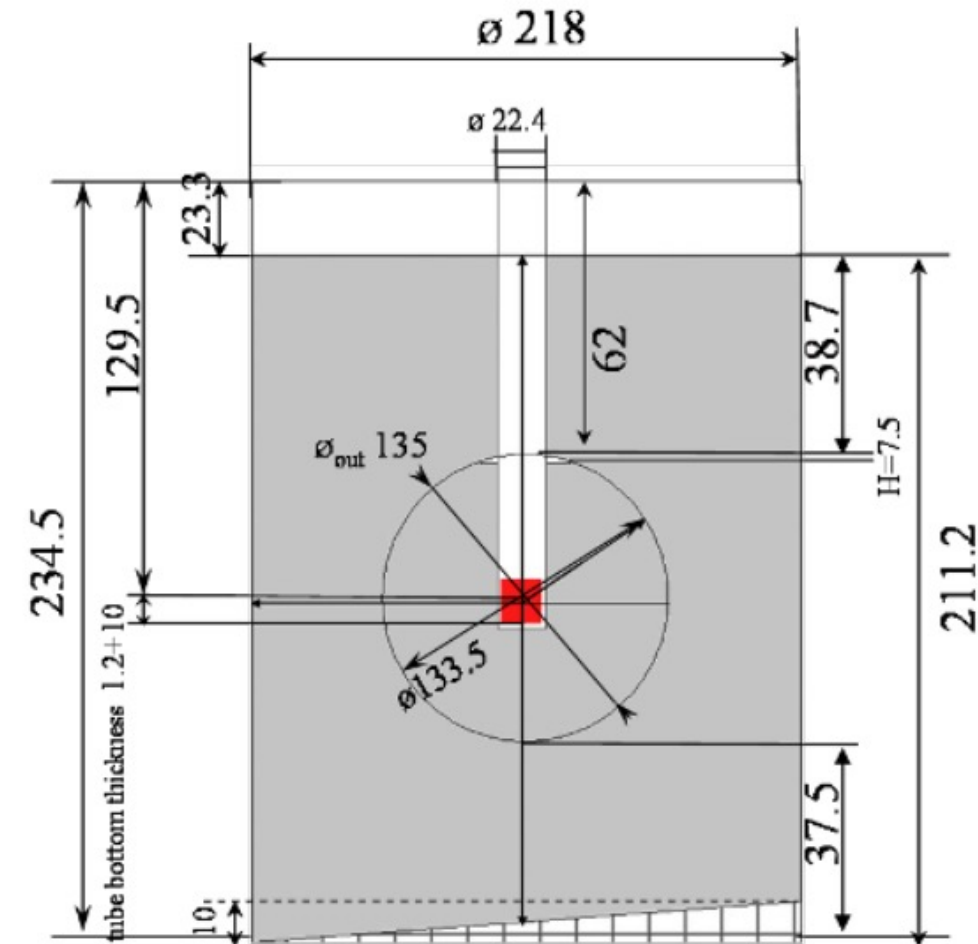
Possible Future Plans

If oscillations, the oscillation length is short (large Δm^2). BEST has poor Δm^2 resolution for values greater than ~2 eV^2.

- Smaller inner volume probably not feasible.
  - Half the volume, need 8x the source strength for same rate.

- ^{65}Zn Source (PRD 97 (2018) 073001)
  - Higher energy source (1.35 MeV vs. 0.75 MeV).
  - Almost twice the cross section.
    - But adds a couple additional excited states.
  - 6-7 kg of enriched ^{64}Zn to produce 0.5 MCi.
  - About 9x longer half life (244 d), many more events even with lower activity.

Regions where inner/outer both about 0.8 of expectation

Sin^{2}2θ = 0.33
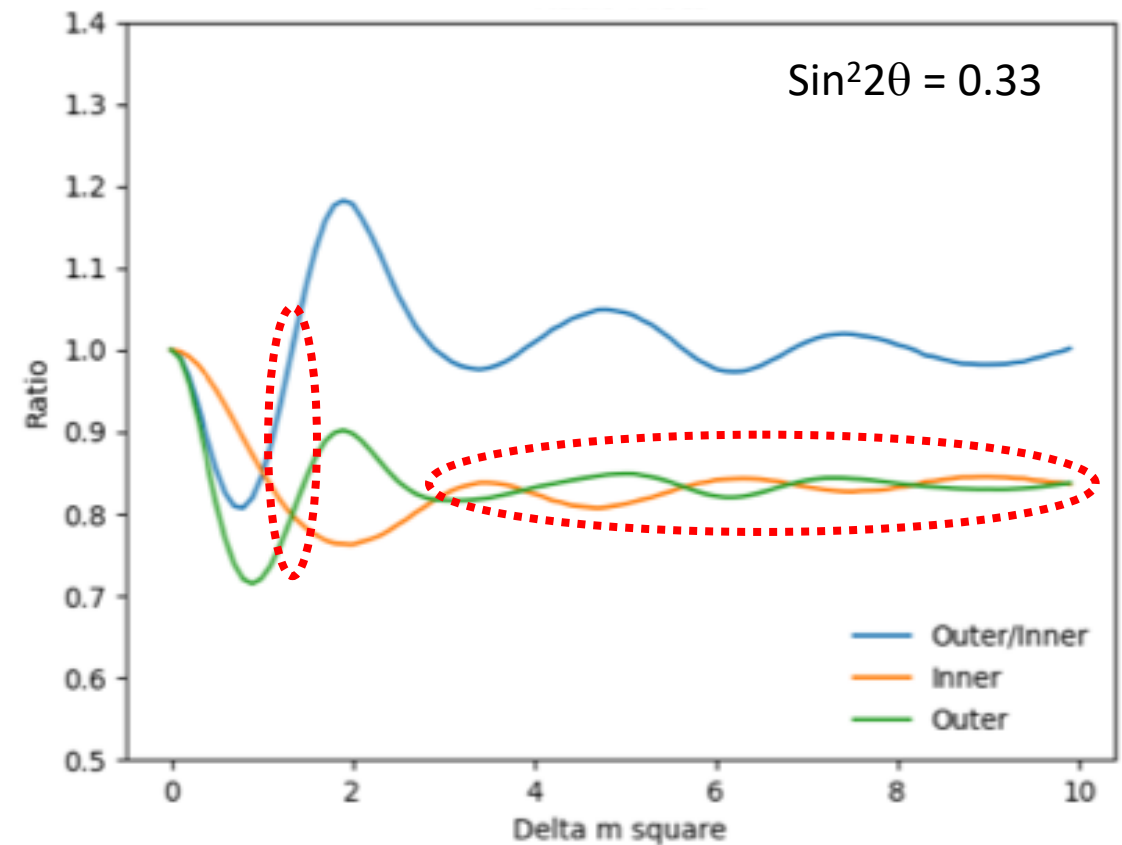
Summary: see arXiv:2109.11482

- BEST measured the ^{71}Ge production in Ga from neutrinos emitted by ^{51}Cr at two distances (inner zone: ~40 cm, outer zone: ~96 cm, but both have large spread.)

- The ratio of the measured-to-predicted rates in both the inner and outer zones are depressed by about 20% from unity. The ratio-of-ratios is ~1.

- The Ga Anomaly is reaffirmed.

- No dependence on oscillation length was observed.
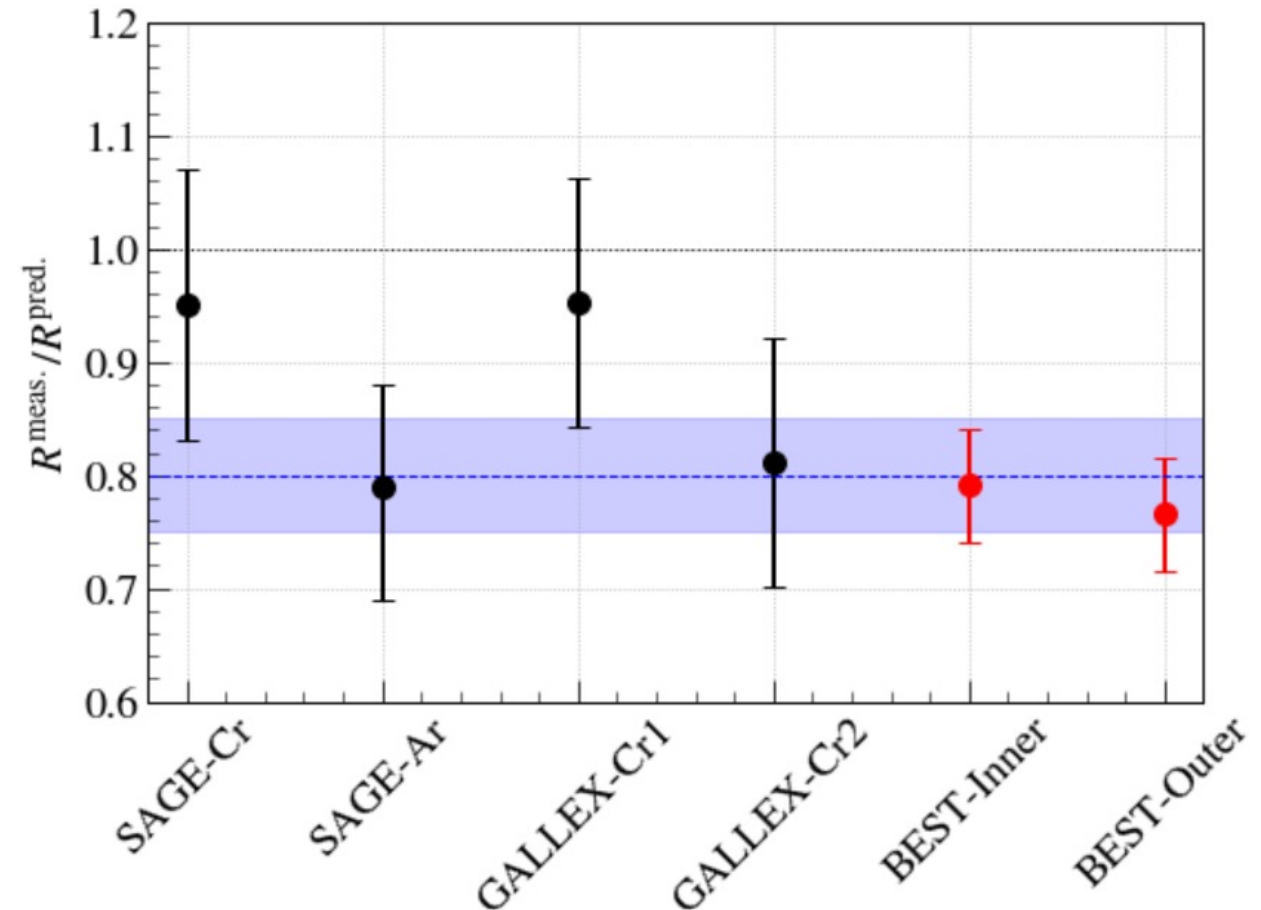
Backups

Counting Results

Inner Zone (a)
Blue=predicted
Red=measured

Outer Zone (a)

Q-Value Measurements

$$\sigma(^{51}Cr) = \sigma_0(^{51}Cr)\left[1 + 0.67\frac{B_1(GT)}{B_0(GT)} + 0.22\frac{B_2(GT)}{B_0(GT)}\right]$$

$$\downarrow$$

$$\sigma_0(^{51}Cr) = F(atom)\frac{1}{ft}$$

$$\downarrow$$
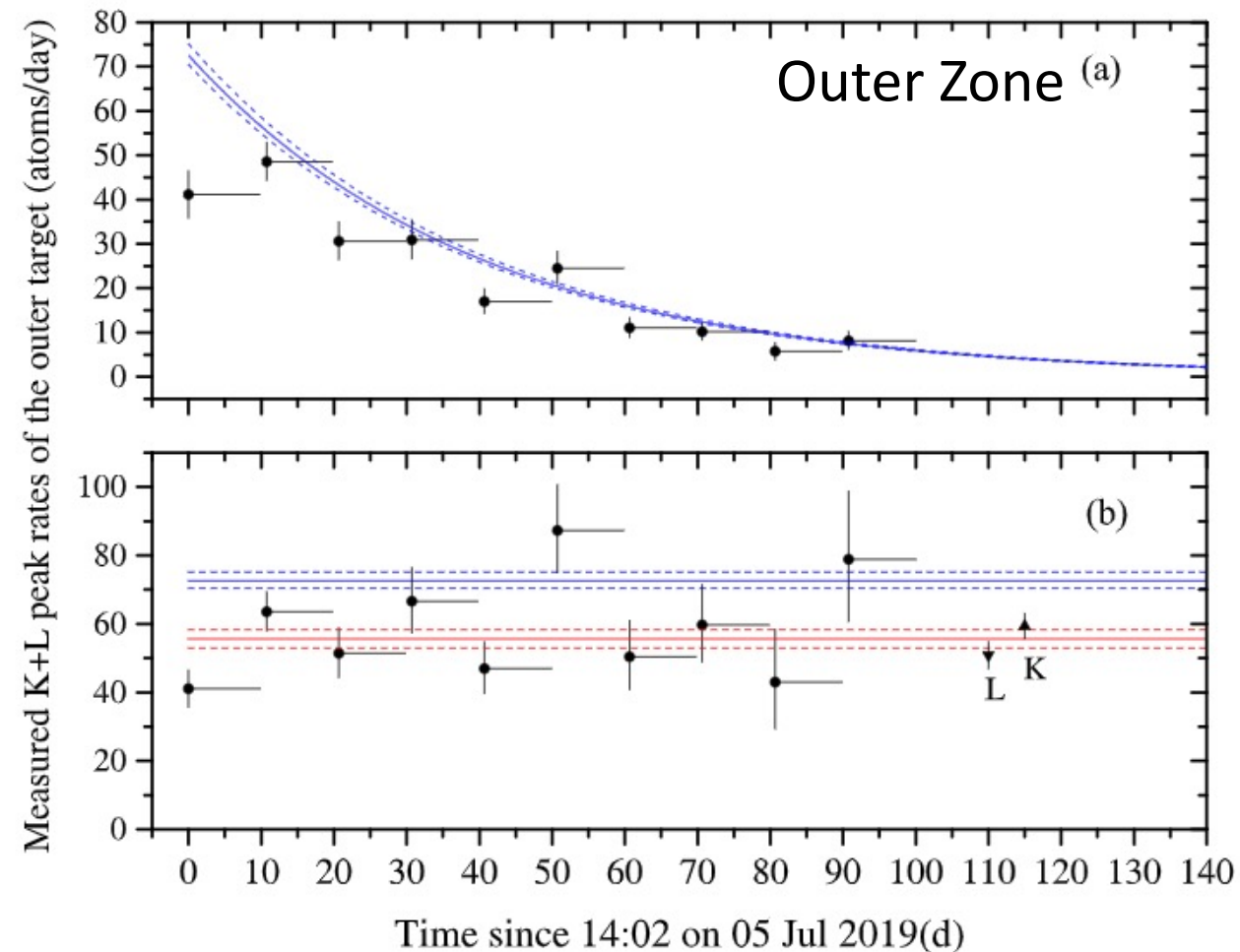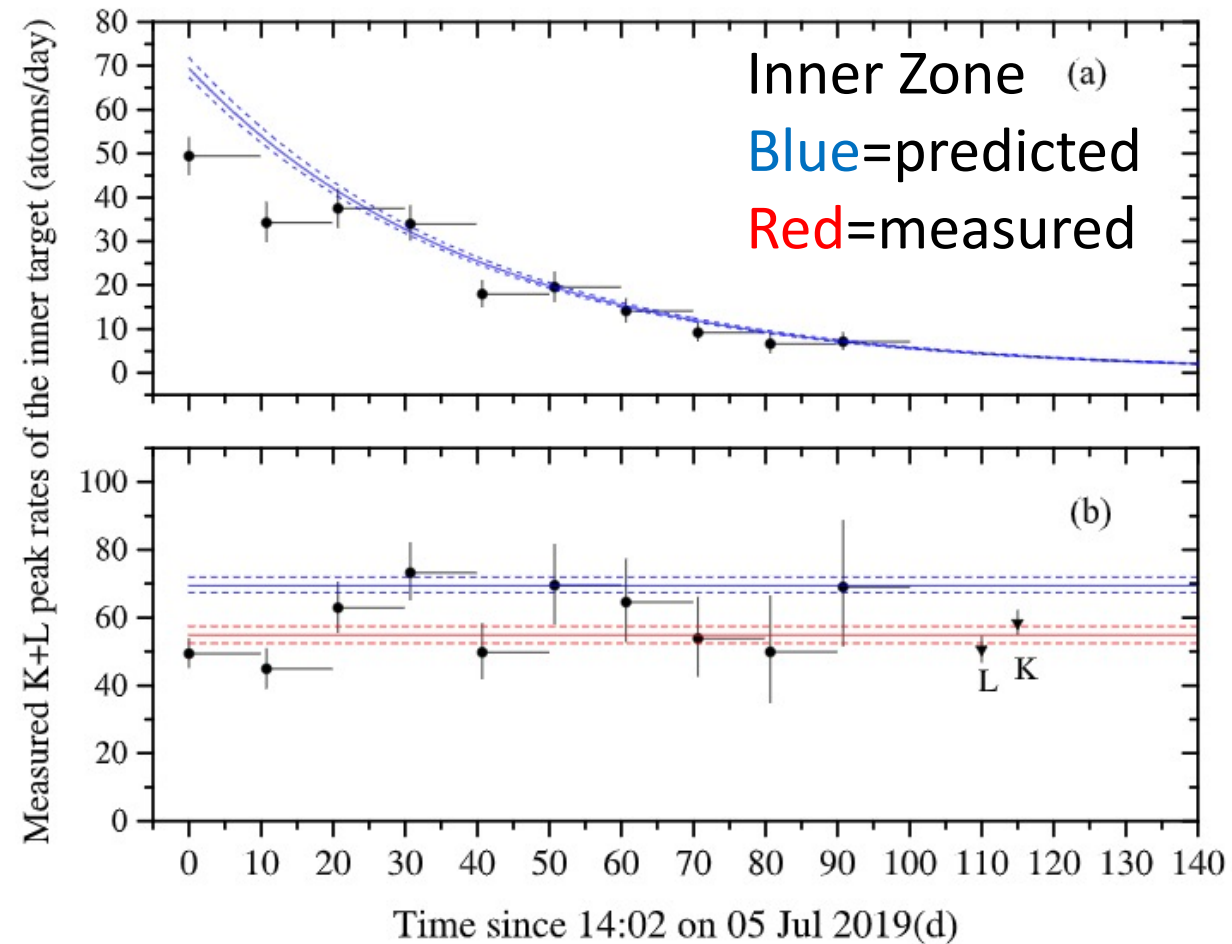
$$ft \propto Q_{EC}^2 \cdot t$$

Penning trap Q-value determination of the $^{71}Ge(\nu,e^-)^{71}Ge$ reaction.
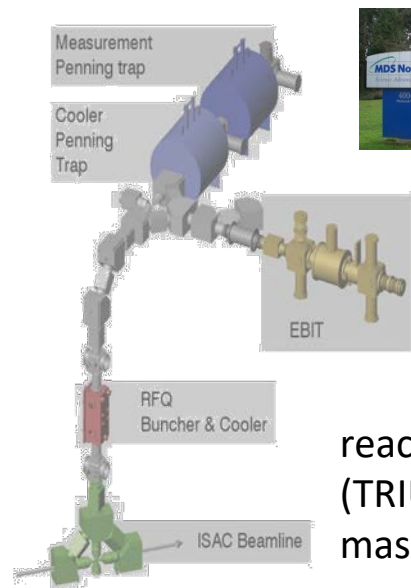
First direct Q-value measurement of the $^{71}Ga(\nu,e^-)^{71}Ge$ reaction was carried out in a Penning trap using the TITAN (TRIUMF's Ion Trap for Atomic and Nuclear science) mass-measurement facility at ISAC/TRIUMF.

Q-value obtained from combined results of the two independent mass-measurement methods is 233.7±1.2 keV, which is in agreement with the previously accepted Q-value for the ν cross-section calculations.

The TITAN result excludes an incorrect Q-value as a cause for the gallium anomaly observed in the GALLEX and SAGE calibration runs.

The TITAN Beamline

Comparison of previous Q-value measurements

Phys. Lett. B 722, 4–5 (2013)
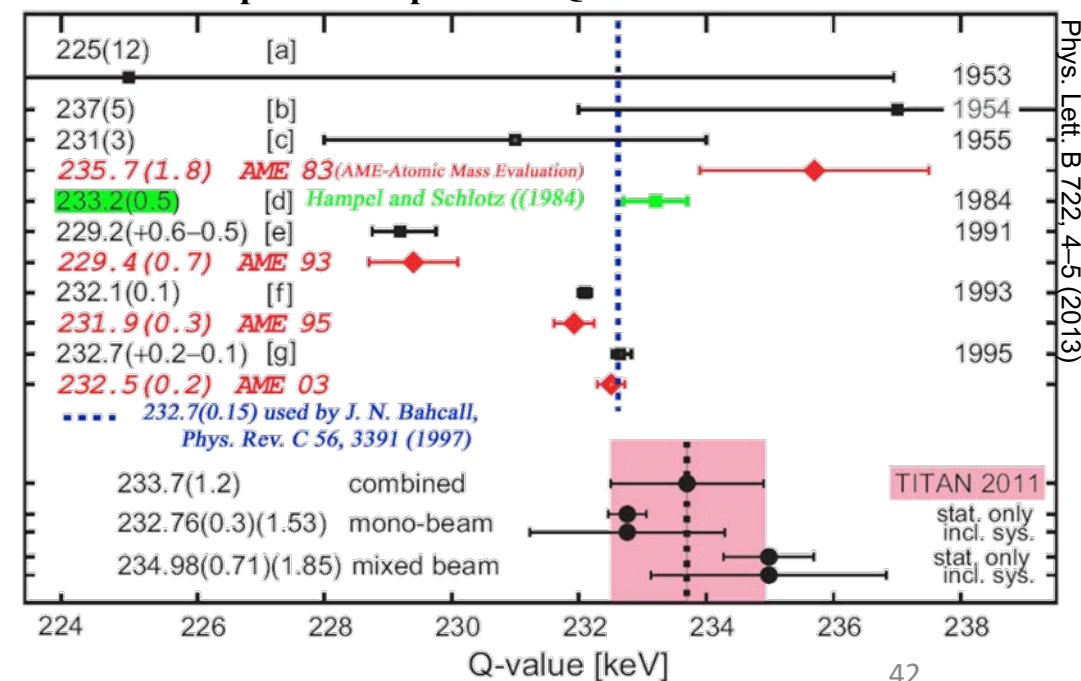
Most Recent Q-Value measurement (Int. J. Mass Spec. 406 (2016) 1)

Result 232.443 ± 0.093
±0.04%

Claims uncontrolled systematic uncertainties were present in TITAN measurements.
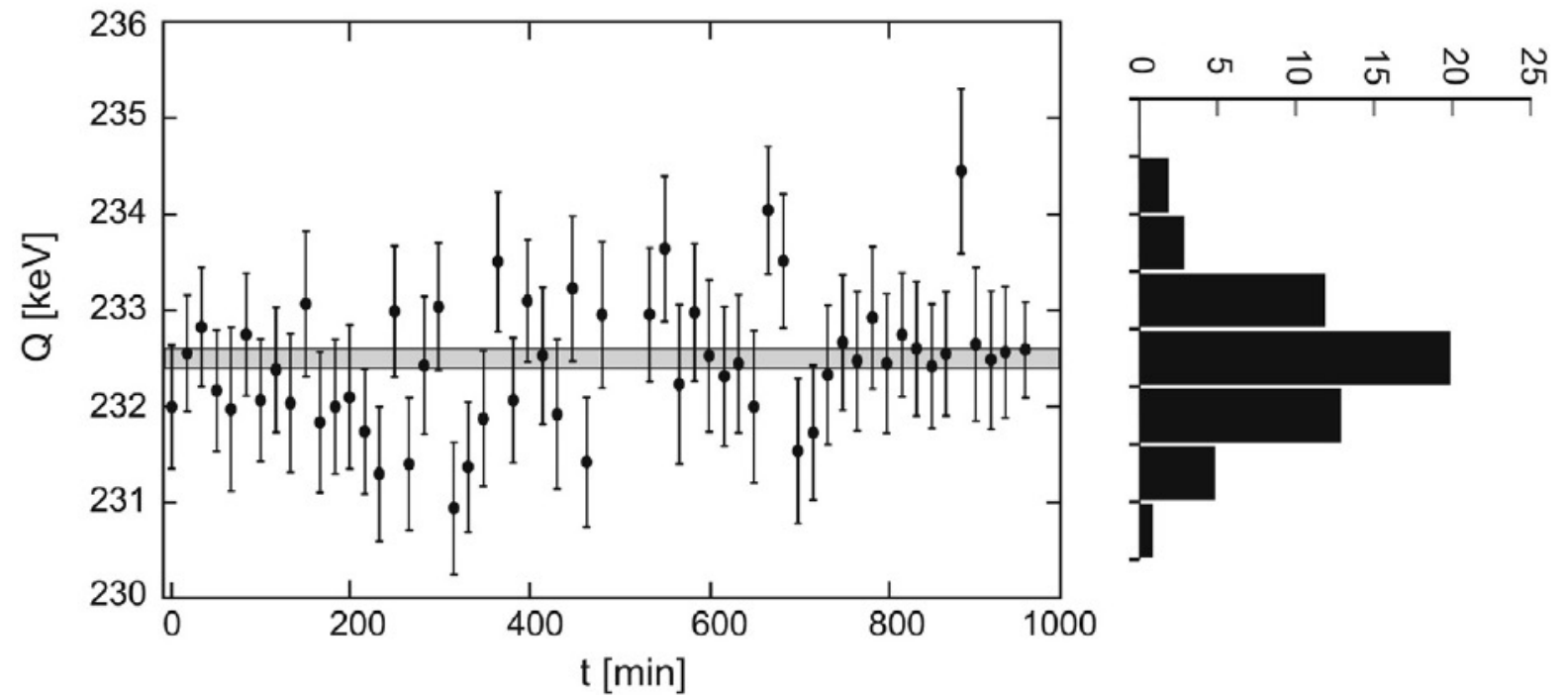
Work on creation of the two-zone reactor for the BEST Ga target

In August-September 2015, two solar measurements were carried out from the BEST gallium target. Extractions and counting of ^{71}Ge atoms were performed independantly for each zone.

The result of the analysis of these measurements is **66.4$^{+28.1}_{-24.3}$** SNU, agrees with the result of the period of measurements 1990 to 2014, **64.6 $\pm$ 2.4** SNU (with statistical uncertainty only).

Exposure and Extraction

| Source exposure				Extraction from cylindrical target		Massa Ga (tons)	Extraction efficiency		Extraction from spherical target		Massa Ga (tons)	Extraction efficiency	
Begin		End											
Dayyear	Mo Da Hr Mn	Dayyear	Mo Da Hr Mn	Name	Date (2019)		from Ga	into GeH4	Name	Date (2019)		from Ga	into GeH4
186.585	07.05 14:02	196.376	07.15 09:02	Cr1	15 Jul 13:59	40.09	0.97	0.91	Cr11	15 Jul 16:01	7.4	0.98	0.93
197.362	07.16 08:41	206.372	07.25 08:56	Cr2	25 Jul 13:51	40.09	0.97	0.92	Cr21	25 Jul 16:32	7.4	0.97	0.92
207.282	07.26 06:47	216.374	08.04 08:59	Cr3	04 Aug 12:47	40.09	0.98	0.97	Cr31	04 Aug 16:37	7.4	0.97	0.92
217.286	08.05 06:52	226.371	08.14 08:54	Cr4	14 Aug 12:51	40.09	0.98	0.94	Cr41	14 Aug 15:35	7.4	0.97	0.92
227.258	08.15 06:12	236.458	08.24 11:00	Cr5	24 Aug 14:35	40.09	1.00	0.97	Cr51	24 Aug 17:17	7.4	0.99	0.96
237.342	08.25 08:13	246.37	09.03 08:51	Cr6	03 Sep 12:35	40.09	1.00	0.98	Cr61	03 Sep 15:18	7.4	1.00	1.00
247.243	09.04 05:50	256.368	09.13 08:50	Cr7	13 Sep 12:29	40.09	1.00	1.00	Cr71	13 Sep 15:11	7.4	1.00	1.00
257.241	09.14 05:47	266.37	09.23 08:52	Cr8	23 Sep 12:32	40.09	1.00	1.00	Cr81	23 Sep 15:17	7.4	1.00	1.00
267.240	09.24 05:46	276.369	10.03 08:51	Cr9	03 Oct 12:27	40.09	0.95	0.88	Cr91	03 Oct 15:00	7.4	0.97	0.92
277.200	10.04 04:49	286.367	10.13 08:48	Cr10	13 Oct 12:26	40.09	0.99	0.95	Cr101	13 Oct 14:59	7.4	0.99	0.94

Source exposure of the two concentric zones
- 10 exposures
- Mean exposure time: 9.18 d
- Masses: 7.4 t (inner) / 40.09 t (outer)

Chemical extraction of ^{71}Ge
- Efficiency is measured by adding a known amount of (inactive) Ge and measuring the mass of extracted Ge
- Amount of added Ge carriers:
  - 2.4 µmol ^{72}Ge (92%); 2.4 µmol ^{76}Ge (95%)
- Mean extraction efficiency from Ga: 98%
- Mean overall efficiency (incl. GeH$_4$ synthesis): 96%
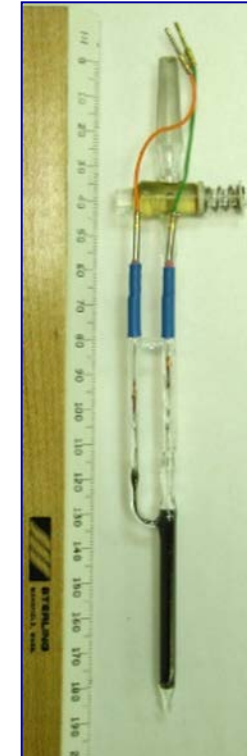
The extracted Ge activity is measured using proportional counters

Systematic Uncertainties

Parameter	Value	Uncertainty
Ga Density ρ (g/cm^3)	6.095	± 0.002
Avogadro's Number N_A (10^{23} atoms Ga/mol)	6.0221	negiligible
Ga molecular weight M (g Ga/mol)	69.72307	± 0.00013
^{71}Ga isotopic abundance f (%)	39.8921	± 0.0062
Atomic Den. $n = \rho N_A f/M$ (10^{22} atoms ^{71}Ga/cm^3)	2.1001	± 0.0008
Source Activity at Ref. Time A (MCi)	3.414	± 0.008
Average Path Length Inner Vol. L_{in} (cm)	52.03	± 0.18
Average Path Length Outer Vol. L_{out} (cm)	54.41	± 0.18
Cross section σ (10^{-45} cm^2)	5.81	$+0.21, -0.16$

Origin of uncertainty	Uncertainty (%)
Chemical extraction efficiency	
Efficiency of extraction from Ga metal	± 1.0
Efficiency of synthesized into GeH$_4$	± 1.3
Carrier carryover	-
Mass of gallium	-
Chemical extraction subtotal	± 1.6
Counting efficiency	
Calculated efficiency	
Volume efficiency	-1.3, +1.5
Peak efficiency	± 1.1
Simulations to adjust for counter filling, Monte Carlo interpolation	± 0.6
Calibration statistics	
Centroid	± 0.1
Resolution	± 0.3
Rise time cut	-
Gain variations	+0.4
Counting efficiency subtotal	-1.5 +1.7
Residual radon after time cuts	-0.05
Solar neutrino background	± 0.20
^{71}Ge carryover	± 0.04
Subtotal	± 0.22
Energy weihting in analysis	± 0.15
Total systematic uncertainty	**-2.5 +2.6**

GALLEX Extraction Efficiency Test (Phys. Lett. B436 (1998) 158)

- GALLEX also did a variety of extraction efficiency tests have been done – all consistent with experimental values.

- A known amount of ^{71}As was added to the Ga. The ^{71}As (2.72 d) decays to ^{71}Ge, which is then extracted and counted. The extraction was 100±1% validating the procedures.

- Rules out 'hot atom' effects.

^{51}Cr Energy Release per Decay (J. Phys.: Conf. Ser. 798 (2017) 012140)

Table 1. The total energy release with Cr-51 decay.

Type of energy release	Energy, keV	Contribution to ^{51}Cr decay	Energy release with ^{51}Cr decay, keV
Gamma rays	320.0835 (4)	0.0991 (2)	31.720 (64)
K-capture	5.465	0.8919 (17)	4.874 (9)
L-capture	0.628	0.0927 (14)	0.0582 (9)
M-capture	0.067	0.0154	0.001
inner bremsstrahlung	751 (max)	$3.8 \times 10^{-4} \times 0.902\ (\pm 10\%)$	0.096 (10)
inner bremsstrahlung	430 (max)	$1.2 \times 10^{-4} \times 0.0983\ (\pm 10\%)$	0.001
Total			36.750 (84) 0.23%

The Calorimeter

1 – MEASUREMENT CELL
a – thermal insulation
b – neutrino source
c – biological shield
d – output thermistor
e – heat exchanger
f – container
g – input thermistor

2 – flow meter
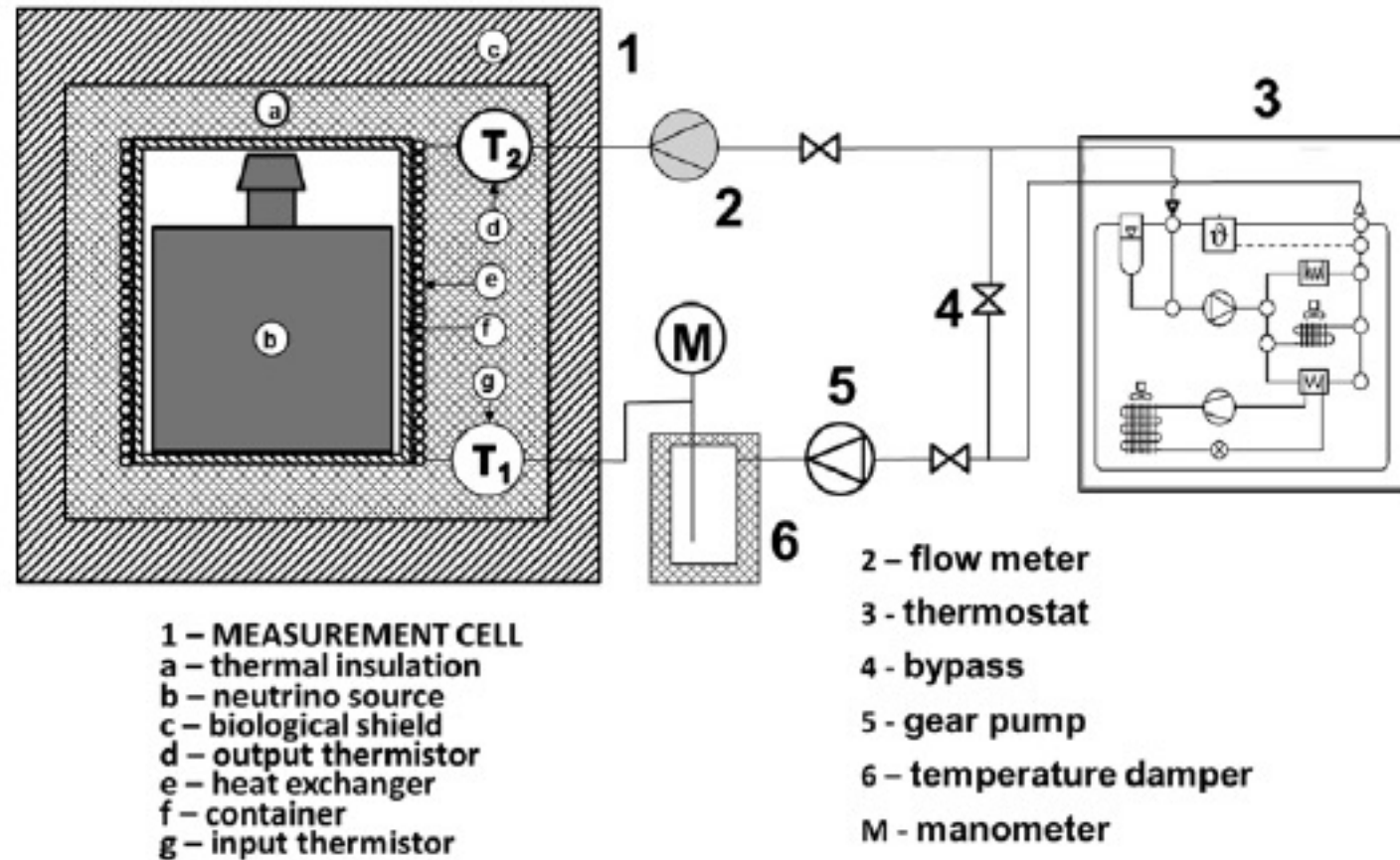3 – thermostat
4 – bypass
5 – gear pump
6 – temperature damper
M – manometer

Figure 1. Hydraulic circuit of the mass flow calorimeter.

2-zone gallium target

Source

Calorimeter

Lead chamber

Biological protection, tangsten

Stainless steel

26 chrome metal disks
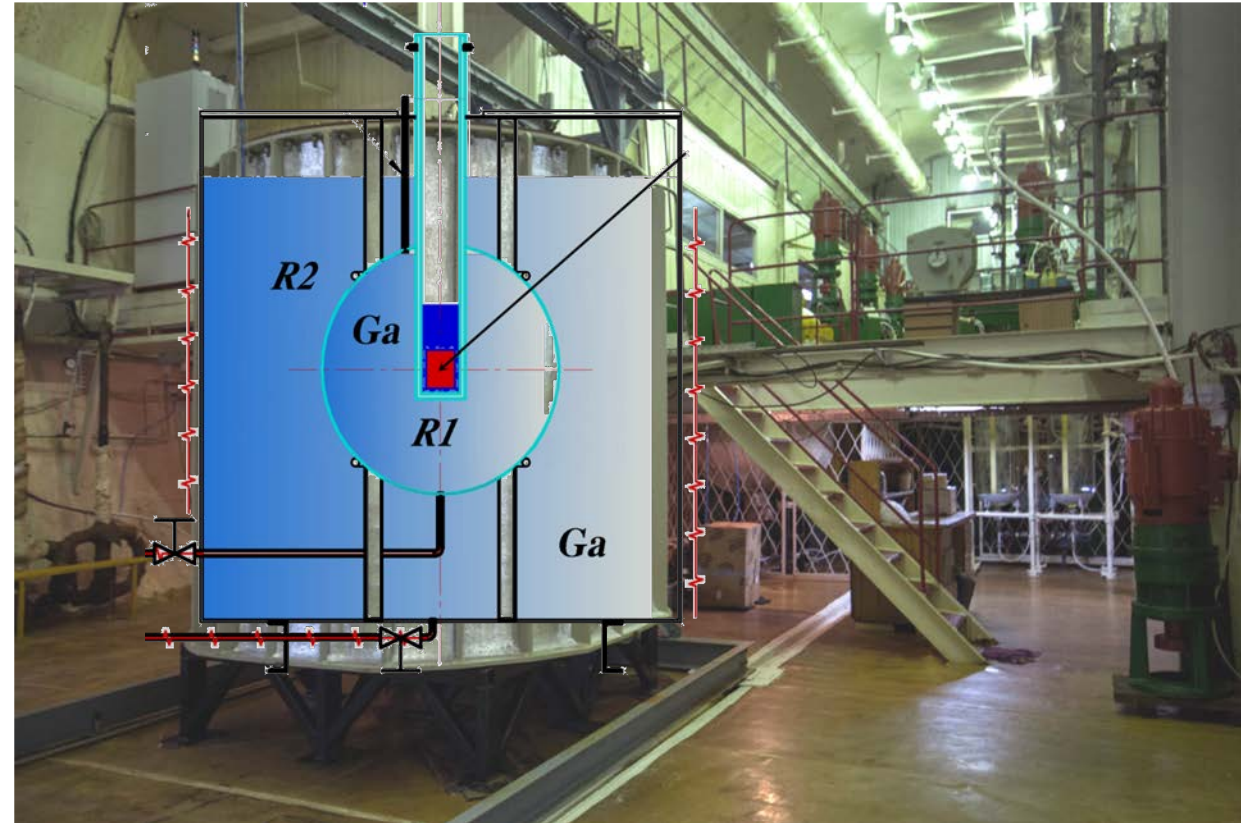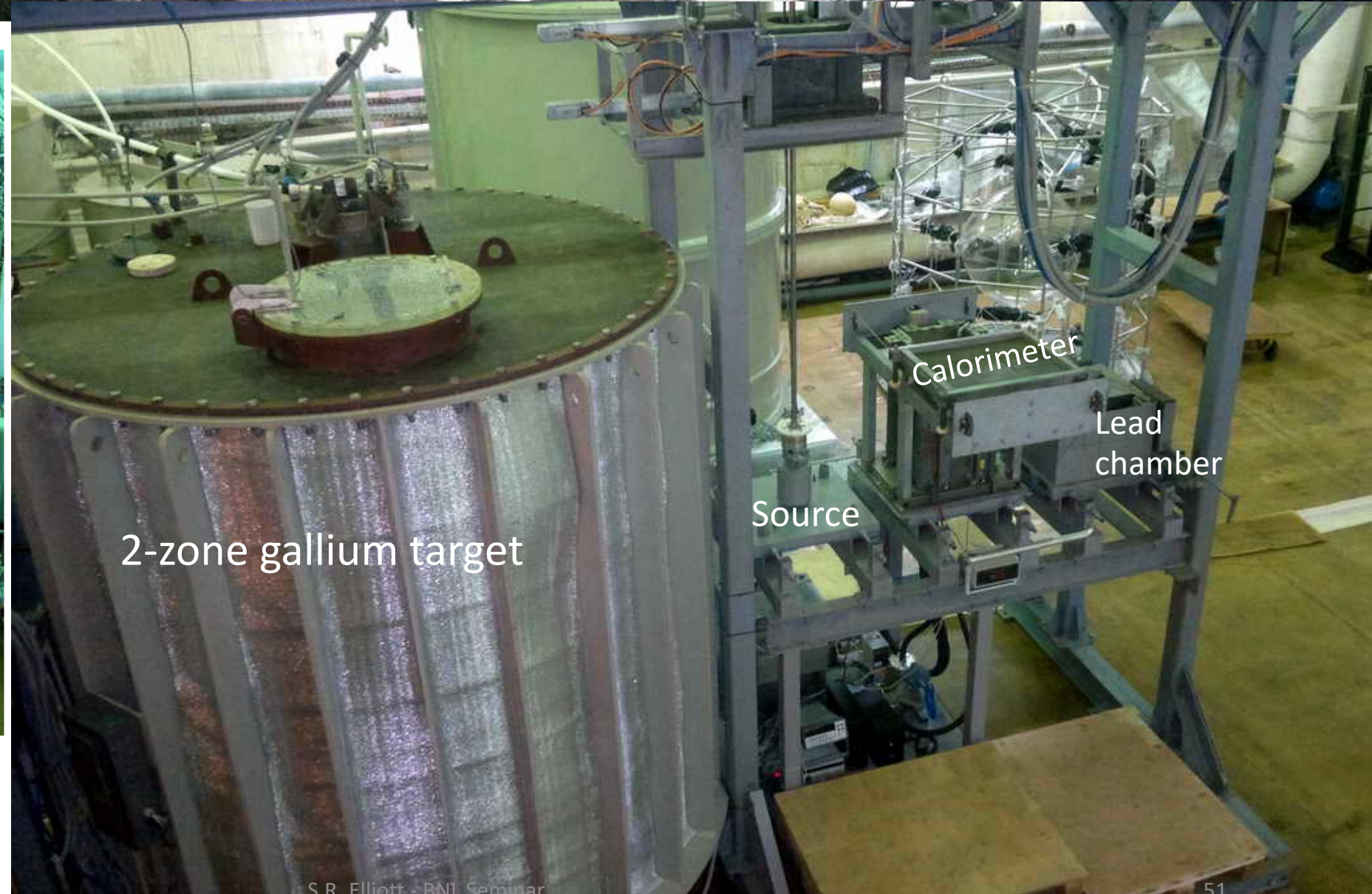
Stainless steel

BEST: Neutrino source

4 kg 97%-enriched ^{50}Cr,
26 Cr metal disks
h = 4 mm, $\varnothing$ 84 and 88 mm.

^{51}Cr (27.7 days)

427 keV ν (9.0%)
432 keV ν (0.9%)

747 keV ν (81.6%)
752 keV ν (8.5%)

320 keV γ
^{51}V (stable)
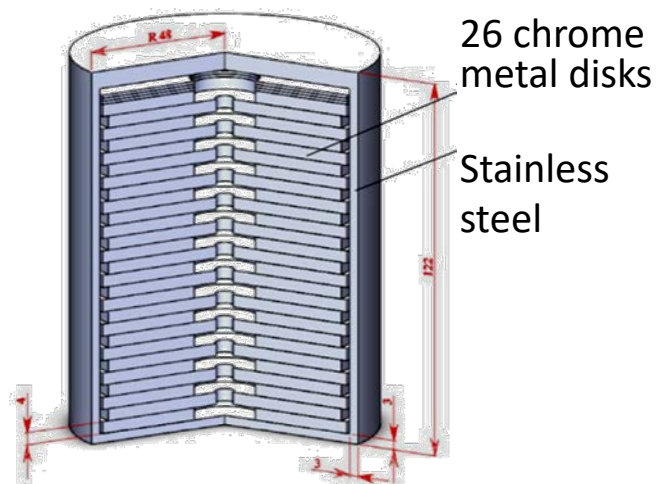
Chromium disks from metallic ^{50}Cr enriched up to 97%.
The enrichment was performed by the JSC "PA "Electrochemical Plant" (Zelenogorsk).
These disks were irradiated for ~100 days with thermal neutrons in the SM-3 reactor (RIAR, Dmitrovgrad). Thermal neutron flux density – 5×10^{15} neutrons /(cm^2 s)

Gamma Ray Spectroscopy of Source

Measured nuclide impurities in the ^{51}Cr source and their contribution to the source activity measurement at the reference time 14:02 on 05.07.2019

Source Gamma Ray Spectrum
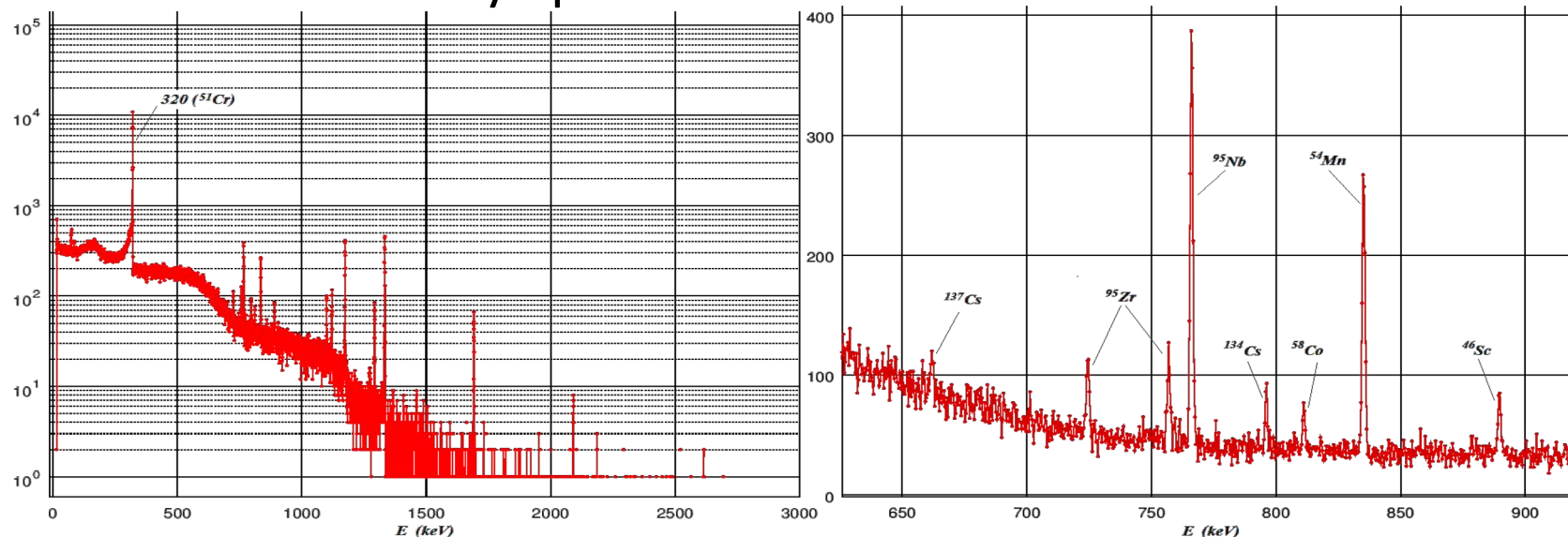
	Isotope, $T_{1/2}$	The energy in the line, keV	The output lines, %	Activity on July 5, mCi	W, mW
1	^{137}Cs, 30.05 y	662	85	8.5×(1±0.23)	0.06
2	^{95}Zr, 64 d	724	11.1	60×(1±0.12)	2.1
		757	54.38		
3	^{95}Nb, 35 d	766	99.8	87×(1±0.04)	
4	^{134}Cs, 2.06 y	796	85.5	3.3×(1±0.18)	0.04
5	^{58}Co, 70.85d	811	99.44	6.0×(1±0.27)	0.08
6	^{54}Mn, 312 d	835	100	13×(1±0.05)	0.1
7	^{46}Sc, 83.8 d	889	100	5.2×(1±0.10)	0.07
		1120	100		
8	^{59}Fe, 44.5 d	1099	57	23×(1±0.07)	0.22
		1291	43.2		
9	^{60}Co, 5.27 y	1173	100	6.6×(1±0.03)	0.11
		1332	100		
10	^{124}Sb, 60.2 d	1690	47.5	5.8×(1±0.06)	0.1
		2091	5.5		
11	^{154}Eu (?), 8.6 y	1274	34.9	0.86×(1±0.18)	0.01
		1595	1.8		
Σ					2.9

From 11 spectrometric measurements of gamma radiation of the source,
- the total amount of heat release from impurity radionuclides is 2.9 ± 0.5 mW , which is ~4·10^{-6} of the initial ^{51}Cr source power, and can be neglected; confirmation of a high purity of the material used to produce the ^{51}Cr source

Pulse Shape Analysis

- 96% acceptance window were verified by separate ^{71}Ge measurements

Counter	Num. Ev. L- all	L-peak T_N cut	Num. Ev L- selected	ratio	Num. Ev. k- all	K-peak T_N cut	Num. Ev k- selected	ratio
sys2z								
YCN43	495	10	463	0.94	489	13.2	468	0.96
YCNA9	1281	13.2	1244	0.97	1167	18.8	1142	0.98
YCN41	1353	10.3	1299	0.96	1434	13.4	1374	0.96
YCN46	941	11.3	897	0.95	865	15.2	837	0.97
mean 2z				0.95				0.97
std				0.01				0.01
sys3								
YCN113	1643	9.1	1626	0.99	1488	13.6	1426	0.96
YCT92	265	13.0	250	0.94	243	17.6	237	0.98
YCT4	508	10.2	497	0.98	328	13.2	313	0.95
YCT3	314	10.3	297	0.95	258	16.4	252	0.98
YCT2	1475	10.1	1415	0.96	1483	16.6	1427	0.96
YCT9	397	9.1	388	0.98	341	14.9	322	0.94
YCT97	1622	11.4	1551	0.96	1607	17.3	1562	0.97
mean sys3				0.96				0.96
std				0.02				0.02

Fit Excluding First Extraction

A fit that excludes the first data point does not change the qualitative conclusion although the statistical significance is decreased.

Inner

Outer
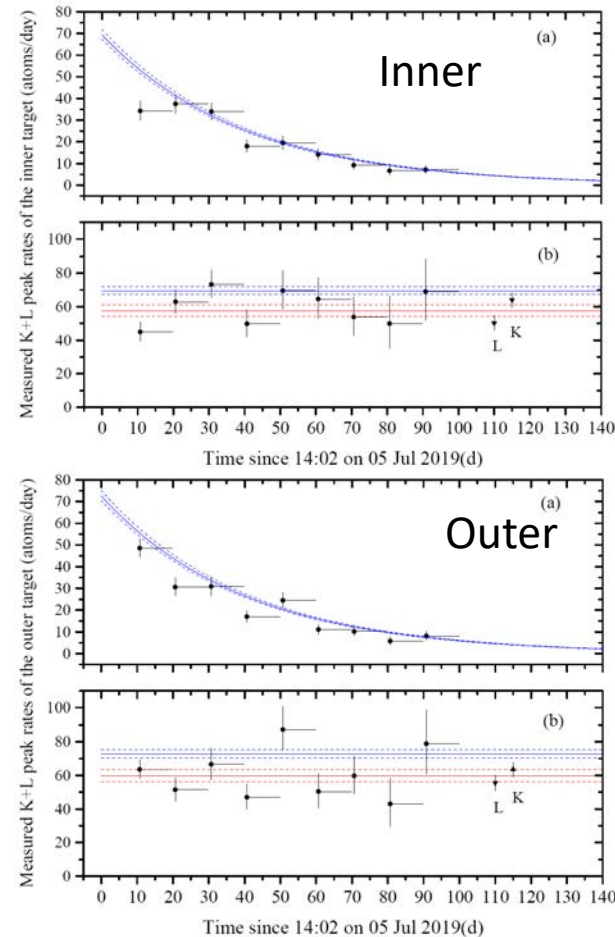
	IN	OUT
Predicted	$69.41^{+2.5}_{-2.0}$	$72.59^{+2.6}_{-2.1}$
Measured	57.7 ± 3.5	59.8 ± 3.6
Ratio	0.83 ± 0.05	0.82 ± 0.06

2.9σ and 3.2σ less than the unity

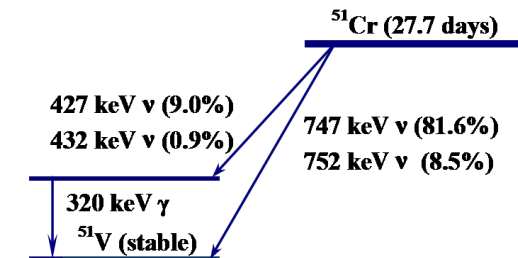$$\text{Note: } \frac{0.83 \pm 0.05}{0.82 \pm 0.06} = 0.99 \pm 0.08$$

Similar deficits observed in both zones

Source Activity – ^{51}Cr Branching Ratio Uncertainty

The calorimetry heat measurement relies on the branching ratio of the 320-keV Cr emission to normalize to activity. If the branching value is in error, so would be the source strength. But the BR is claimed to be known to a precision much smaller than our result, 0.1%. Even so, would not explain Ar result.

ENDF data

E(decay)	E(level)	$I\varepsilon^{\dagger\ddagger}$	Log ft	Comments
(432.37 *21*)	320.0835	9.930 *10*	5.8631 *7*	εK=0.8910; εL=0.09347; εM+=0.01556
(752.45 *21*)	0.0	90.070 *10*	5.3910 *3*	εK=0.8919; εL=0.09268; εM+=0.01541

^{51}Cr (27.7 days)

427 keV v (9.0%)
432 keV v (0.9%)
747 keV v (81.6%)
752 keV v (8.5%)

320 keV γ

^{51}V (stable)

Specific Results

Ref	branch	method
Nucl. Phys. A423 (1984) 121	0.1030(19)	Counting neutrons and gamma rays in (p,n)
NIM A 339 (1994) 20	0.0990(8)	NaI – absolute activity ???
NIM A 339 (1994) 20	0.1008(11)	Ge – absolute activity ???
Applied Radiation and Isotopes 68 (2010) 596	0.0987(3)	Beta-gamma coincidence (Ge-based)
Applied Radiation and Isotopes 62 (2005) 63	0.099(1)	Si(Li) with fixed activity

56
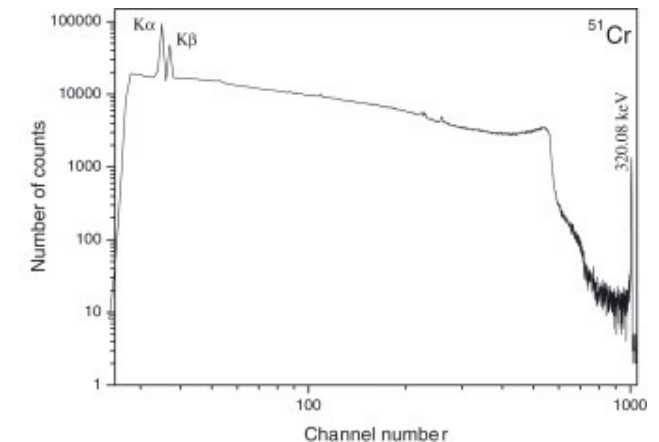
Cross Section – Energy of ^{51}Cr Neutrinos

- Cross section scales approximately as neutrino energy squared.

- Q value is well known: 0.1%. So no more than about 0.2% on cross section

- The energies of the emitted neutrinos are taken from the decay Q value and specific K/L shell energies.

- A full calculation of the final atomic state should be pursued. If the shell is altered during the decay, the energy of that state will not be shared with the neutrino.

- Maybe a keV decrease in neutrino energy…
  - 1 keV out of 750 is about 1.3%, cross section might decrease by maybe 2.5%.
  - Too small to explain difference.

- Would have to do similar calculation for Ar.

Cross Section – Electron Density at the Nucleus

- The ground state cross section for ^{71}Ga-> ^{71}Ge is derived from the decay rate of ^{71}Ge.

- The decay rate is proportional to $|M|^2|\psi(0)|^2$, where $\psi(0)$ is the electron density at the nucleus. If the theoretical $\psi(0)$ is estimated high, the cross section would be underestimated.

- The cross section, however, only needs the matrix element $|M|^2$.

- Hence a calculation of $\psi(0)$ is used to convert the decay rate to a cross section.

- Experimental tests of $\psi(0)$ measure the ratio of electron capture to positron decay.

  - For ^{22}Na, measurement is ±1%, but disagrees with theory by 6%. (Appl. Rad. Iso. 134 (2018) 225)
  - But theory is high wrt experiment, so effect seems to be in wrong direction to be an explanation.
  - Need a better experimental test, and hopefully with A near 71 (^{68}Ga?)
  - Will need complementary calculations.

Cross Section – Electron Density at the Nucleus

Concern raised by
RGH Robertson

- The ground state cross section for ^{71}Ga-> ^{71}Ge is derived from the decay rate of ^{71}Ge and the electron density at the nucleus

$$\sigma_0 = \frac{1.2429 \times 10^{-47} \text{ cm}^2}{\Sigma_i q_i^2 g_i^2}$$

q_i: $E_{threshold}$-$E_{binding,i}$
g_i^2: square of the radial wavefunction
[PRC **56**, 3391 (1997)]

Rev. Mod. Phys. **49**,1 (1977)

Exp./Theor. of P_K

- For this calculation, g_i^2 is only calculated, not measured

- Experimental tests of g_i^2 measure the ratio of electron capture to positron decay (EC/β+)
  - $P_{EC}/P_{\beta+} = (P_K+P_L)/P_{\beta+} = P_K/P_{\beta+} (1+P_L/P_K)$
  - $\sigma(P_L/P_K)\sim \pm3\%$, $\sigma(P_K)\sim \pm5\%$ Rev. Mod. Phys. **49**,1 (1977)
  - (EC/β+)$_{theory}$ systematically *higher* than (EC/β+)$_{exp.}$ (see figure on the right).
  - For most nuclides, effect is in the opposite direction to the Ga anomaly
  - For ^{22}Na, measurement is ±1%, but disagrees with theory by 5%. (Appl. Rad. Iso. 134 (2018) 225)
  - Need a better experimental test, and hopefully with A near 71 (^{68}Ga?)
  - Will need complementary calculations.

Exp./Theor. of (EC/β+)
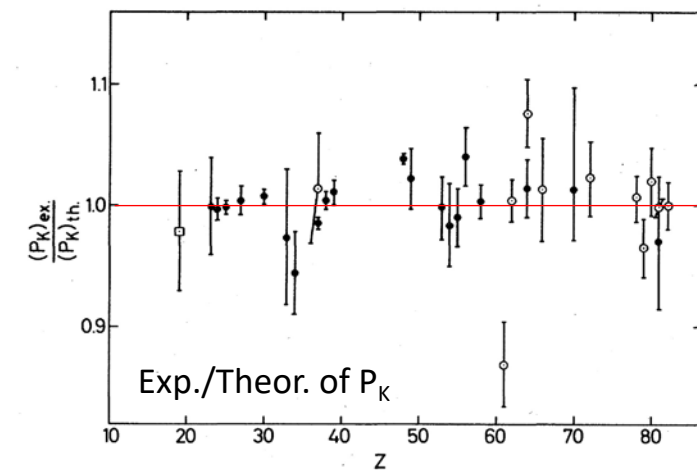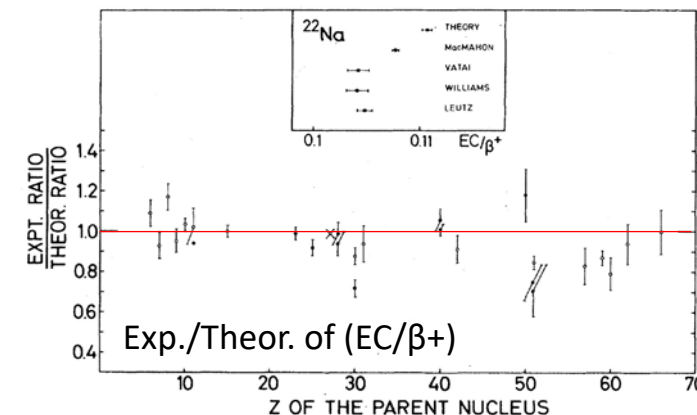
EC/β+ Ratio Near A=71   Rev. Mod. Phys. **49**,1 (1977)

Nuclide	Z	A	K/β+ Theory	K/β+ Exp.	Ratio (Exp./Theory)	Ref.
Zn	30	65	30.5±0.4	27.7±1.5	0.908	Hammer (1968)
Ga	31	68	1.36±0.03	1.28±0.12	0.941	Ramaswamy (1959)

Nuclide	Z	A	EC/β+ Theory	EC/β+ Exp.	Ratio (Exp./Theory)	Ref.
Zn	30	65	34.5±0.04	24.9±1.5	0.722	Sehr (1954)
Na*		22	0.1143±0.001	0.1083±0.009	0.948	Mougeot (2018)

* Included here as it is the most studied nuclide for EC/β+ Ratio

Ga-Solar Neutrino Experiments

- Bahcall   Book   132(20) SNU
  P_{ee} solar ~ 60% (SNO) , **56% (SAGE PRC)**   =74 (11)

- SAGE   PRC 80 (2009) 015807   65+-6

- GALLEX(new) PLB 685 (2010) 47   67+-7

Agreement is good but only to about 10% or so. Doesn't support or refute Ga Anomaly.

Comparison of Measured pp Flux: SAGE, Borexino

Table 2 | Borexino experimental solar-neutrino results

Nature 562 (2018) 505

Solar neutrino	Rate (counts per day per 100 t)	Flux (cm^{-2} s^{-1})	Flux–SSM predictions (cm^{-2} s^{-1})	
pp	$134 \pm 10^{+6}_{-10}$	$(6.1 \pm 0.5^{+0.3}_{-0.5}) \times 10^{10}$	$5.98(1.0 \pm 0.006) \times 10^{10}$	(HZ)
			$6.03(1.0 \pm 0.005) \times 10^{10}$	(LZ)

PHYSICAL REVIEW C **80**, 015807 (2009)

Dividing this capture rate by the cross section for capture of pp neutrinos from Table III gives the measured electron neutrino pp flux at Earth of

$$\phi^{\oplus}_{pp} = 3.38(1^{+0.14}_{-0.14}) \times 10^{10}/(\text{cm}^2 \text{ s}). \qquad (18)$$

If we use Eq. (7) and the value of $\langle P^{ee}_i \rangle = 0.561(1^{+0.030}_{-0.042})$ from Table III then the pp flux produced in the Sun is

$$\phi^{\odot}_{pp} = 6.0(1 \pm 0.14) \times 10^{10}/(\text{cm}^2 \text{ s}). \qquad (19)$$

Our present result for the pp flux is in good agreement with the previous estimates that we have made during the past 6 years

The two experiments claim similar pp fluxes, about 15% or so. Not precise enough to exclude or confirm overall efficiency as explanation of the Ga anomaly.

Wilk's Theorem in Question

- In our analysis for the oscillation parameters, the test statistic is assumed to be χ^2 distributed (Wilk's theorem)

- However, Wilk's theorem is in doubt when: EPJ.C **80**, 750 (2020), EPJ.C **81**, 2 (2021)

  - The population of likelihood function occurs near the parameter space edge. But our result is not near the boundary.

    - Physical bound at $\sin^2 2\theta \geq 0$

  - There is a degeneracy in parameter space

    - Δm^2 becomes undefined when $\sin^2 2\theta \rightarrow 0$

    - $\sin^2 2\theta$ becomes unphysical when $\Delta m^2 \rightarrow 0$
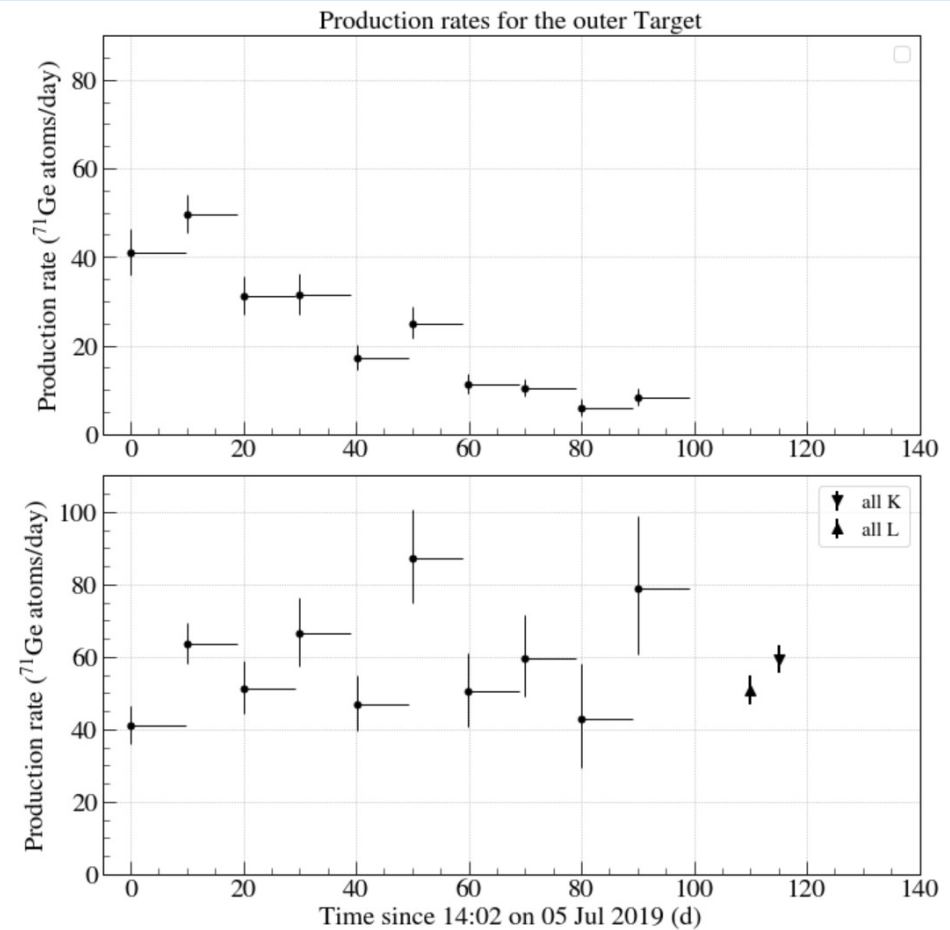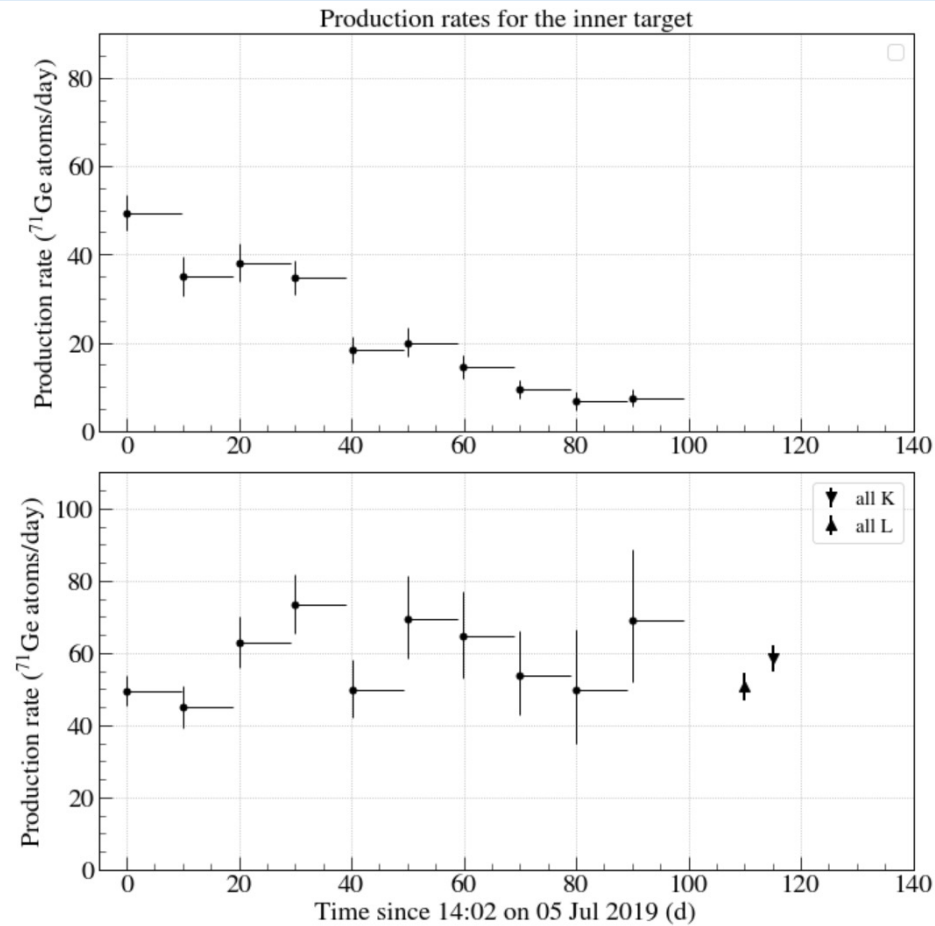
  The test statistic *a priori* significantly deviates from a χ^2 distribution

- A recent study found no significant difference between Wilk's and a Feldman-Cousins analysis for the BEST results.
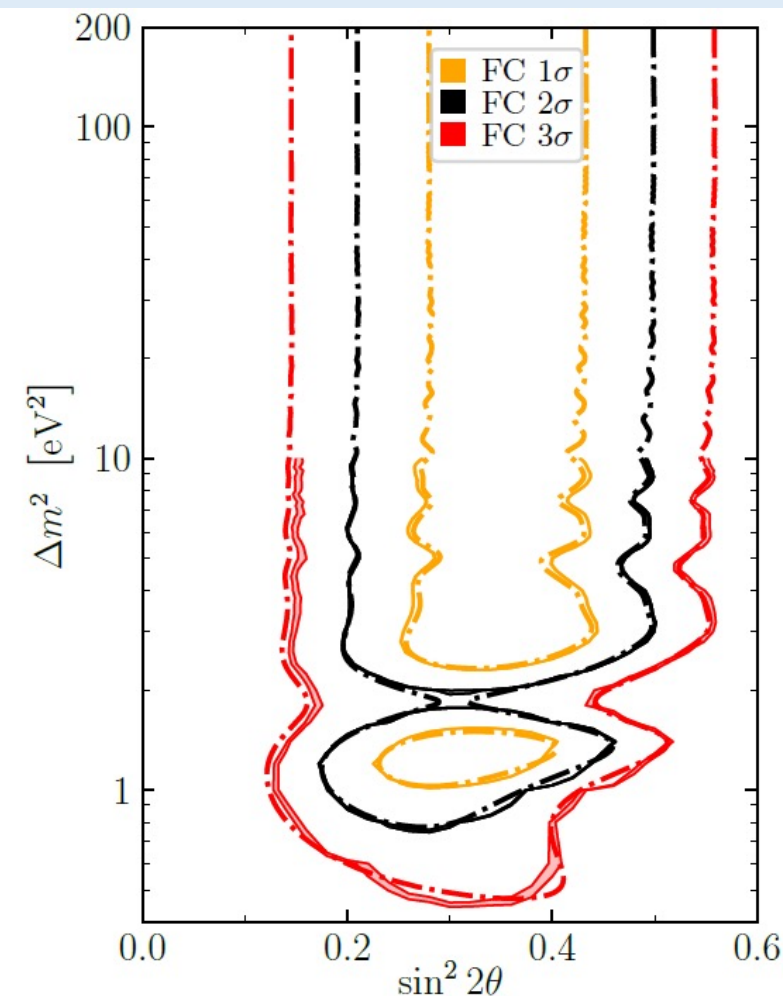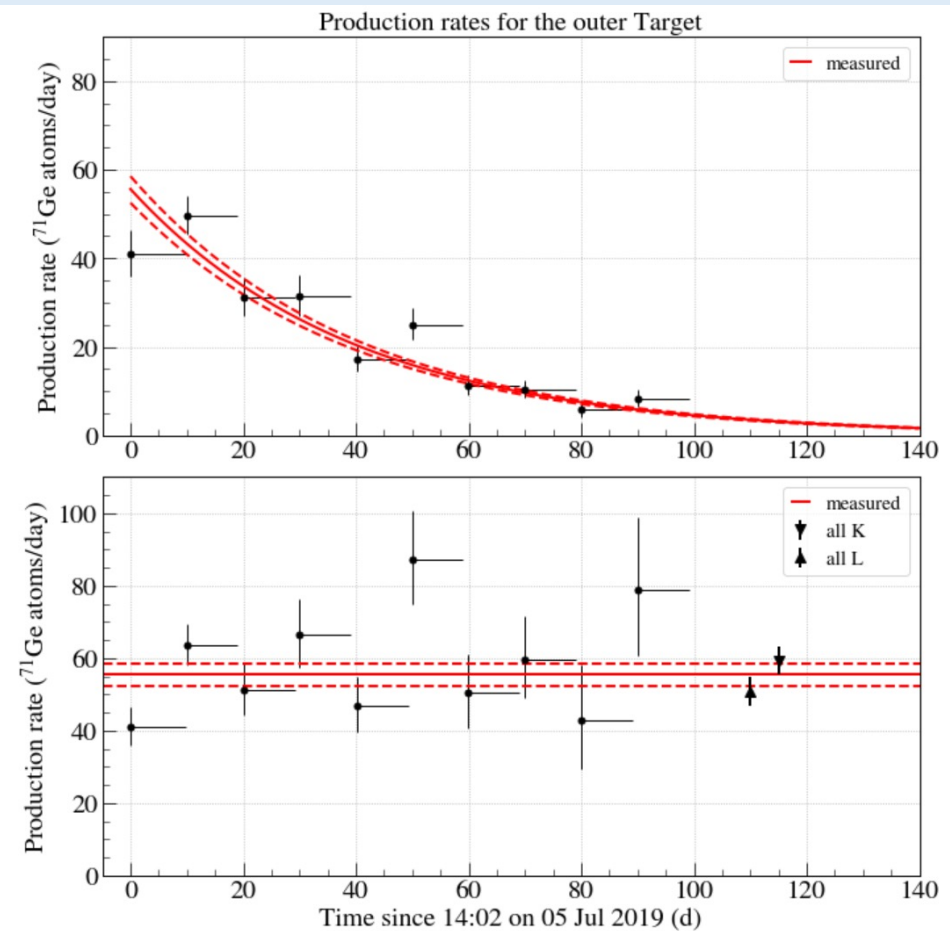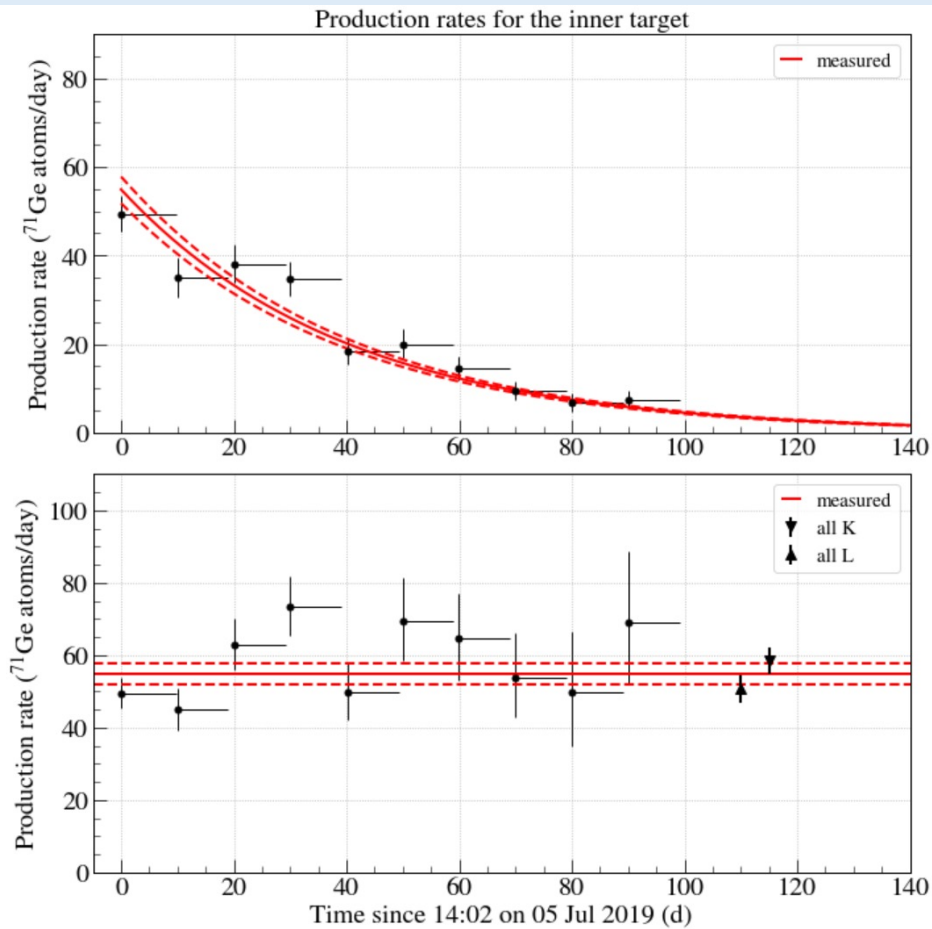
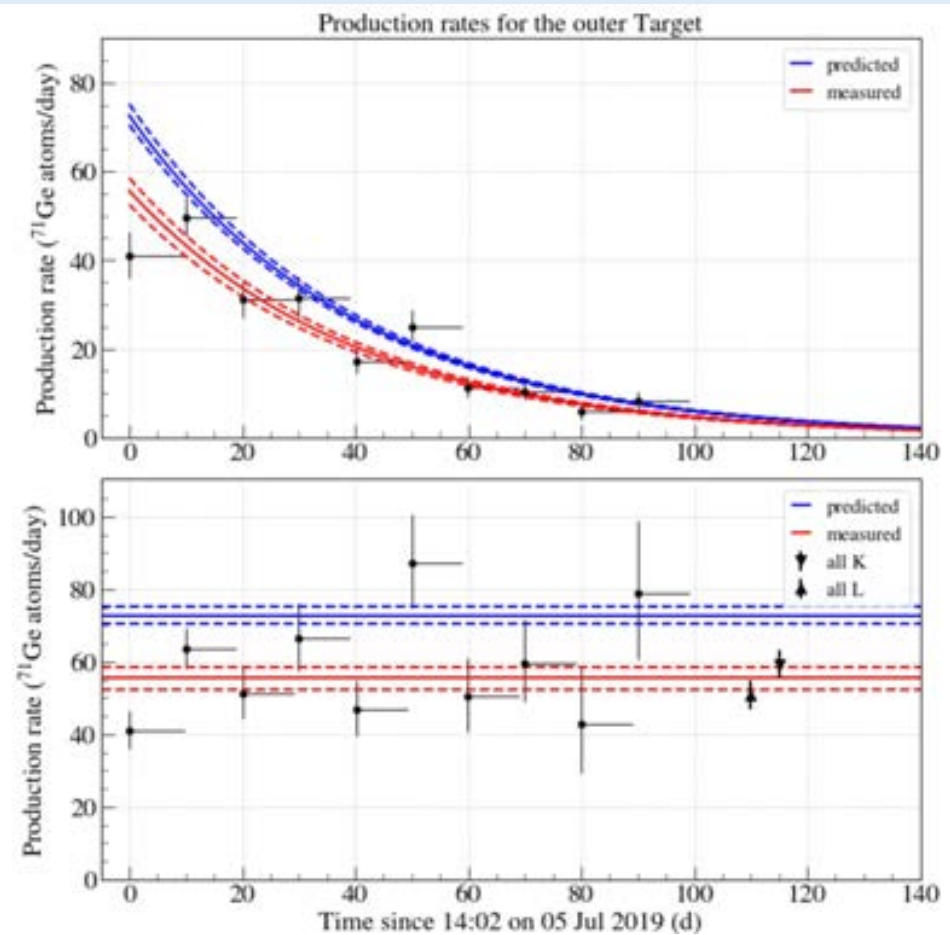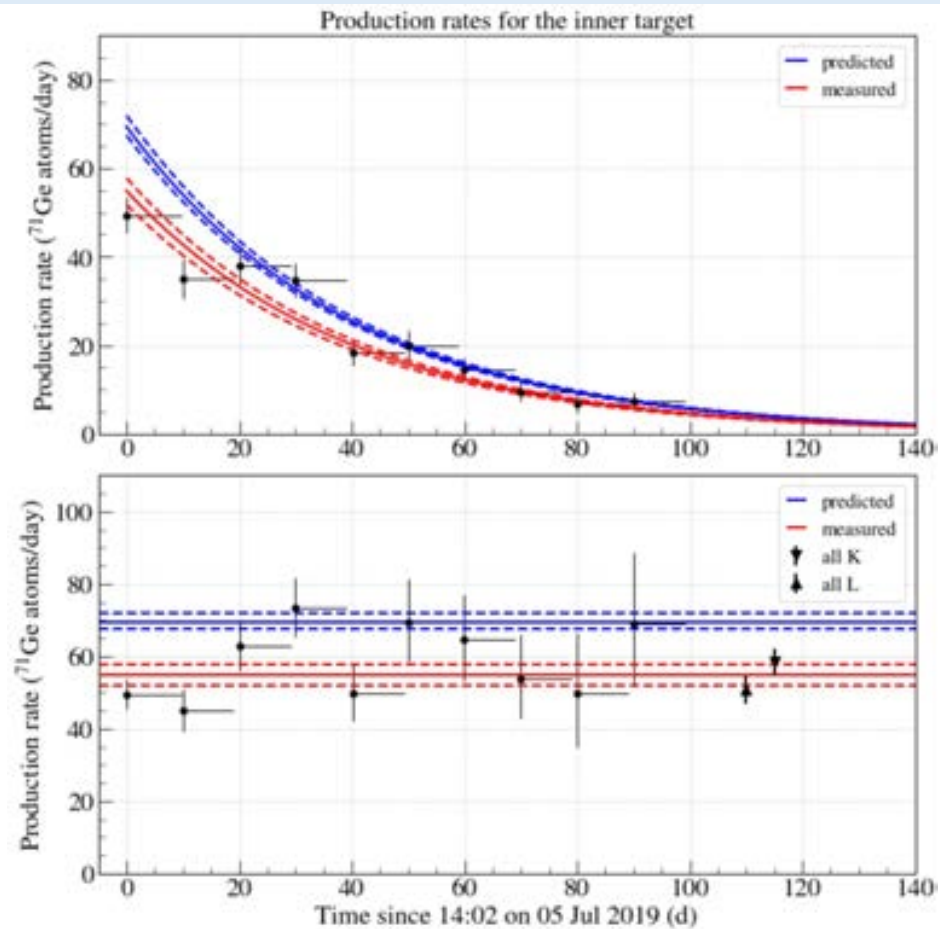Wilk's (dotted) vs Feldman-Cousins (solid). Analysis by arXiv:2111.12530.

Counting Results

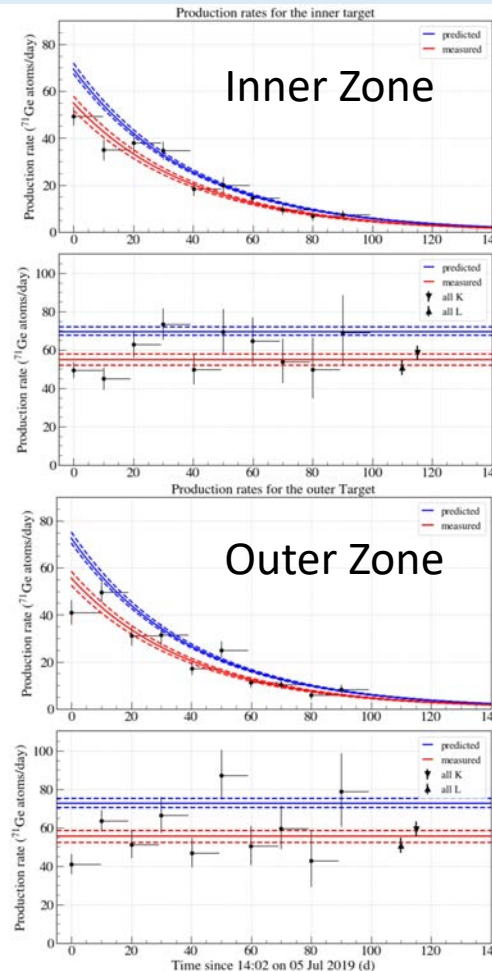# Counting Results

Counting Results

Predicted vs. Measured Production Rates

K+L-peak

Extraction	Number of candidate events	Number fit to ^{71}Ge	^{51}Cr source production	Solar ν production	Carryover	^{71}Ge Production decay rate (atoms/day)
Inner-1	180	176.3	175.5	0.8	0.0	$49.4^{+4.0}_{-4.2}$
Inner-2	129	111.5	107.7	0.8	3.1	$44.9^{+5.6}_{-5.9}$
Inner-3	132	117.6	115.3	0.7	1.6	$62.9^{+7.1}_{-7.4}$
Inner-4	93	87.3	85.6	0.6	1.1	$73.3^{+8.0}_{-8.6}$
Inner-5	134	60.2	58.4	0.6	1.2	$49.8^{+7.7}_{-8.2}$
Inner-6	81	48.8	47.7	0.4	0.7	$69.5^{+11.0}_{-12.0}$
Inner-7	91	45.0	43.9	0.5	0.6	$64.6^{+11.6}_{-12.6}$
Inner-8	59	33.6	32.4	0.6	0.6	$53.8^{+11.0}_{-12.2}$
Inner-9	106	23.7	22.7	0.6	0.4	$49.9^{+14.9}_{-16.5}$
Inner-10	88	25.2	24.3	0.6	0.3	$69.1^{+17.3}_{-19.4}$
Comb. K+L	1093	724.0	708.2	6.1	9.7	$54.9^{+2.4}_{-2.5}$

K+L-peak

Extraction	Number of candidate events	Number fit to ^{71}Ge	^{51}Cr source production	Solar ν production	Carryover	^{71}Ge Production decay rate (atoms/day)
Outer-1	181	133.4	129.6	3.7	0.1	$41.1^{+5.2}_{-5.3}$
Outer-2	174	163.8	158.6	3.3	1.9	$63.6^{+5.5}_{-5.7}$
Outer-3	116	92.5	88.2	2.8	1.5	$51.4^{+6.9}_{-7.3}$
Outer-4	98	82.3	78.9	2.5	0.8	$66.6^{+9.2}_{-9.8}$
Outer-5	120	64.0	59.5	3.5	1.0	$46.9^{+7.2}_{-7.9}$
Outer-6	97	62.3	59.3	2.6	0.4	$87.3^{+12.3}_{-13.2}$
Outer-7	69	38.0	34.4	3.2	0.4	$50.4^{+9.6}_{-10.6}$
Outer-8	68	43.4	39.2	3.9	0.4	$59.7^{+10.8}_{-11.7}$
Outer-9	66	20.2	17.0	3.0	0.2	$43.0^{+13.5}_{-15.3}$
Outer-10	81	31.8	28.0	3.6	0.2	$78.8^{+18.1}_{-20.0}$
Comb. K+L	1069	738.8	699.8	32.2	6.8	$55.6^{+2.6}_{-2.7}$

Production rates for the inner target

Inner Zone

Production rates for the outer Target

Outer Zone

Time since 14:02 on 05 Jul 2019 (d)

	IN	OUT
Predicted	$69.41^{+2.5}_{-2.0}$	$72.59^{+2.6}_{-2.1}$
Measured	54.9 ± 2.9	55.6 ± 3.1
Ratio	0.791 ± 0.05	0.766 ± 0.05

4.2σ and 4.8σ less than the unity

$$\text{Note: } \frac{0.77 \pm 0.05}{0.79 \pm 0.05} = 0.97 \pm 0.07$$

Similar deficits observed in both zones

Likelihood Fits (Inner)

Likelihood Fits (Outer)